Long-wavelength thermocapillary instability with the Soret effect

A. Oron[1,*] and A. A. Nepomnyashchy[2]
[1]*Department of Mechanical Engineering, Technion-Israel Institute of Technology, Haifa 32000, Israel*
[2]*Department of Mathematics and Minerva Center for Nonlinear Physics of Complex Systems, Technion-Israel Institute of Technology, Haifa 32000, Israel*

(Received 11 June 2003; published 30 January 2004)

We study the onset of Marangoni instability of the quiescent equilibrium in a binary liquid layer with a nondeformable interface in the presence of the Soret effect. Linear stability analysis shows that both monotonic and oscillatory long-wavelength instabilities are possible depending on the value of the Soret number χ. Sets of long-wavelength nonlinear evolution equations are derived for both types of instability. Bifurcation analyses reveal that in the regime of monotonic instability square patterns bifurcate supercritically and they are preferred in competition with roll patterns. Hexagonal patterns bifurcate transcritically and the condition for the emergence of steady stable hexagonal patterns is derived. In the case of oscillatory instability, traveling and standing waves are found to bifurcate supercritically in the narrow range of the Soret parameter and traveling waves are found to become the selected type of flow.

DOI: 10.1103/PhysRevE.69.016313 PACS number(s): 47.20.−k, 47.20.Dr, 47.20.Ky

I. INTRODUCTION

Various transport processes encountered in technology and nature are owing to or affected by simultaneous action of temperature and solute concentration gradients. Different configurations of those gradients were discussed [1] in the context of buoyancy-driven convection. Similar settings can be also considered in regards with the surface-tension-driven convection in the no-gravity environment. Relevant examples are different techniques of materials processing, e.g., crystal growth, from binary or multicomponent liquid mixtures. Many of them, especially those employing the floating zone and temperature-gradient methods, involve large temperature and possibly concentration gradients imposed in various directions relatively to the melt [1].

The buoyancy-driven (Rayleigh) convection in a binary mixture has been a subject of an extensive investigation, in both the theoretical and experimental aspects. It is now well known that simultaneous presence of two or more components with different diffusivities in a liquid layer may lead to a variety of new phenomena. Specifically, if two or more components with different diffusivities are present in a fluid and their gradients make opposing contributions to the fluid density, a possible source of instability can be created. For instance, a layer subjected to a stabilizing solute concentration can exhibit an oscillatory instability when a destabilizing thermal gradient across it opposes the former [2]. Under some conditions, the characteristic spatial scale of convective patterns is large. In that case a long-wavelength asymptotic approach can be applied [3]. Two main physical situations are possible here: (i) the temperature gradient and the concentration gradient have independent sources (double-diffusive convection); (ii) the temperature gradient is imposed, while the concentration gradient is generated spontaneously due to the Soret effect. Extensive reviews [4,5] encompass the work on double-diffusive phenomena and their applications in oceanography, chemistry, metallurgy, geology, geophysics, etc. For a review on the convection in layers of a binary liquid with the Soret effect the reader is referred to Ref. [6].

If the liquid layer has a free surface, the surface-tension-driven (Marangoni) convection, caused by the dependence of surface tension on both the temperature and the solute concentration, can appear. In a majority of mixtures surface tension decreases with temperature and increases (decreases) with concentration of an inorganic (organic) solute. Therefore, if a layer of a binary mixture is subjected to both temperature and concentration gradients, nonuniformities of those at the free surface lead to the emergence of surface shear stresses that can under certain conditions destabilize the quiescent base state.

There is a significant amount of research done on the Marangoni instability in a pure fluid layer [7]. However, to the best of our knowledge the literature is scarce with a research on double-diffusive and Soret effects in the context of interfacial phenomena. Linear stability analysis of the quiescent equilibrium in a layer with a free surface under the action of independent temperature and concentration gradients across the layer was carried out by Castillo and Velarde [8–10] and by McTaggart [11]. It was found that when both the thermal and solutal Marangoni numbers are positive, i.e., the shear stresses induced separately by thermal and concentration components enhance each other, the quiescent state can lose its stability monotonically. However, when the corresponding Marangoni numbers have opposite signs, i.e., when the shear stresses induced separately by thermal and solutal components counteract, the instability is mostly oscillatory. The case where the solute concentration gradient is produced by the Soret effect was considered in Refs. [12–15]. A specific type of oscillatory instability due to the excitation of capillary-gravity waves by the Marangoni effect was discovered in Ref. [16].

Investigations of nonlinear aspects of the Marangoni convection in binary liquids are much more rare. Ho and Chang

*Corresponding author. FAX: 972-4-829-5711. Email address: meroron@tx.technion.ac.il

[17] analyzed, by means of amplitude equations, the flow dynamics in the neighborhood of the double-zero point, i.e., a point in the space of parameters where monotonic and oscillatory instabilities compete. Bergeon *et al.* [18] studied numerically the two-dimensional (2D) Marangoni convection in binary mixtures in a container. Recently, 3D oscillatory convective regimes were studied by Bestehorn and Colinet [19] by direct numerical simulations of the hydrodynamic equations, as well as on the basis of the model complex Swift-Hohenberg equation. Let us mention also the experimental work [20] devoted to the combined Rayleigh-Marangoni convection in a binary solution. Linear and nonlinear analyses of long-wavelength coupled double-diffusive thermocapillary instability were carried out by Braverman and Oron [21]. The nonlinear theory of the long-wavelength monotonic Marangoni instability in a pure liquid was developed in Refs. [22–26]. In the case of the oscillatory instability we refer to the nonlinear theories developed for the buoyancy convection in a binary fluid in Refs. [27–29].

It is the purpose of the present work to study the important case of convection in a binary liquid layer with *poorly conducting boundaries*, where the quiescent state is unstable with respect to *long-wavelength* disturbances. Here, in the limit when the heat flux across the layer is fixed, uniform variations of the temperature and of the solutal concentration are neither damped nor amplified. When large-scale horizontal modulation of both the temperature and concentration fields is imposed, flows are generated by the surface-tension gradients which can lead to a long-wavelength instability. In the present paper we first carry out the linear stability analysis of the system and find both long-wavelength monotonic and oscillatory modes of instability in various parameter domains. The long-wavelength nonlinear analysis is performed next to derive sets of evolution equations for both the monotonic and oscillatory Marangoni instabilities in a binary liquid in the presence of the Soret effect. The obtained equations are then used for the analysis of pattern selection.

II. STATEMENT OF THE PROBLEM AND GOVERNING EQUATIONS

We consider a layer of an incompressible binary liquid of an infinite extent in the longitudinal directions x^* and y^* and thickness d lying on a rigid plane and exposed to the ambient gas phase at its nondeformable free surface. The layer is subjected to a transverse temperature gradient, $-a, a>0$. It is assumed that the film is sufficiently thin, so that the effect of buoyancy can be neglected as compared to the impact of the Marangoni effect. The Soret effect is assumed to be present. Surface tension σ is assumed to be dependent upon both temperature T^* and solute concentration C^*, $\sigma=\sigma(T^*,C^*)$, and therefore thermocapillary and solutocapillary effects are taken into account.

We now proceed to the formulation of the mathematical model used in what follows. A set of governing equations in the presence of the Soret effect and when static gravity is incorporated into the pressure terms is given by

$$\boldsymbol{\nabla}\cdot\mathbf{v}^*=0, \tag{1a}$$

$$\mathbf{v}^*_{t^*}+(\mathbf{v}^*\cdot\boldsymbol{\nabla})\mathbf{v}^*=-\rho^{-1}\boldsymbol{\nabla}p^*+\nu\nabla^2\mathbf{v}^*, \tag{1b}$$

$$T^*_{t^*}+\mathbf{v}^*\cdot\boldsymbol{\nabla}T^*=\kappa\nabla^2T^*, \tag{1c}$$

$$C^*_{t^*}+\mathbf{v}^*\cdot\boldsymbol{\nabla}C^*=D\nabla^2C^*+\alpha D\nabla^2T^*. \tag{1d}$$

Here $\mathbf{v}^*$, T^*, p^*, and C^* are fields of the fluid velocity, temperature, pressure, and solute concentration, respectively, ν, κ, D, and α are, respectively, kinematic viscosity, thermal diffusivity, mass diffusivity of the mixture, ρ is its reference and the Soret coefficient, density, $\boldsymbol{\nabla}\equiv(\partial_{x^*},\partial_{y^*},\partial_{z^*})$, and t^* is time.

The boundary conditions at the bottom rigid surface reflect the no-slip condition for the velocities, a specified heat flux and mass impermeability, respectively,

$$\mathbf{v}^*=0,\quad T^*_{z^*}=-a,\quad C^*_{z^*}=\alpha a\quad\text{at}\quad z^*=0. \tag{2}$$

At the free nondeformable surface the boundary conditions are, respectively, the kinematic boundary condition, heat transfer governed by the Newton's law of cooling, and mass impermeability:

$$\mathbf{v}^*\cdot\mathbf{e}_z=0,\quad kT^*_{z^*}+q(T^*-T^*_\infty)=0,$$

$$kC^*_{z^*}-\alpha q(T^*-T^*_\infty)=0\quad\text{at}\quad z^*=d, \tag{3}$$

where k is the thermal conductivity of the mixture, q is the rate of heat transfer by convection at the free surface, $\mathbf{e}_z$ is the unit vector in the z^* direction, and T^*_∞ is the sustained temperature of the ambient gas phase. Also, the balance of tangential stresses at the free surface is given by

$$\mu\partial_{z^*}\mathbf{u}^*=\boldsymbol{\nabla}_\perp\sigma, \tag{4}$$

where $\nabla_\perp\equiv(\partial_{x^*},\partial_{y^*})$ and $\mathbf{u}^*$ is the projection of vector $\mathbf{v}^*$ onto the plane normal to $\mathbf{e}_z$. Under the assumption of linear dependence of surface tension σ on both temperature and concentration

$$\sigma(T^*,C^*)=\sigma_0-\sigma_t(T^*-T^*_r)+\sigma_c(C^*-C^*_r),$$

Eq. (4) is rewritten in the form

$$\mu\partial_{z^*}\mathbf{u}^*=-\sigma_t\boldsymbol{\nabla}_\perp T^*+\sigma_c\boldsymbol{\nabla}_\perp C^*\quad\text{at}\quad z^*=d, \tag{5}$$

wherein $\sigma_t=-\partial\sigma/\partial T^*$, $\sigma_c=\partial\sigma/\partial C^*$, $\mu=\nu\rho$ is the fluid viscosity, and T^*_r and C^*_r are, respectively, the reference temperature and concentration. For most aqueous solutions of inorganic salts surface tension decreases with temperature and increases with salt concentration, hence the values of σ_t and σ_c are positive for this choice of a mixture. For aqueous solutions of organic solutes surface tension usually decreases with concentration, and therefore in this case σ_c will be negative.

We define the dimensionless variables of the problem as

$$t^*=\frac{d^2}{\nu}t,\quad(x^*,y^*,z^*)=d(x,y,z),\quad(\mathbf{u}^*,\mathbf{v}^*)=\frac{\kappa}{d}(\mathbf{u},\mathbf{v}),$$

$$T^* = T^*_\infty + adT, \quad C^* = \frac{\sigma_t a d}{\sigma_c} C, \quad p^* = \frac{\rho \nu \kappa}{d^2} p. \tag{6}$$

This yields the dimensionless form of the governing equations

$$\boldsymbol{\nabla} \cdot \mathbf{v} = 0, \tag{7a}$$

$$\mathbf{v}_t + P^{-1}(\mathbf{v} \cdot \boldsymbol{\nabla})\mathbf{v} = -\boldsymbol{\nabla} p + \nabla^2 \mathbf{v}, \tag{7b}$$

$$PT_t + \mathbf{v} \cdot \boldsymbol{\nabla} T = \nabla^2 T, \tag{7c}$$

$$SC_t + L^{-1}\mathbf{v} \cdot \boldsymbol{\nabla} C = \nabla^2 C + \chi \nabla^2 T, \tag{7d}$$

and the boundary conditions are rewritten as

$$\mathbf{v} = \mathbf{0}, \quad T_z = -1, \quad C_z = \chi \quad \text{at} \quad z = 0, \tag{7e}$$

$$\mathbf{v} \cdot \mathbf{e}_z = 0, \quad T_z + BT = 0, \quad C_z - \chi BT = 0,$$

$$\partial_z \mathbf{u} + M \boldsymbol{\nabla}(T - C) = 0 \quad \text{at} \quad z = 1. \tag{7f}$$

Here

$$P = \frac{\nu}{\kappa}, \quad S = \frac{\nu}{D}, \quad \chi = \frac{\alpha \sigma_c}{\sigma_t}, \quad B = \frac{qd}{k},$$

$$M = \frac{\sigma_t a d^2}{\mu \kappa}, \quad \text{and} \quad L^{-1} = \frac{S}{P} \tag{8}$$

are, respectively, the Prandtl, Schmidt, Soret, Biot, Marangoni, and inverse Lewis numbers. It should be emphasized that in virtually all physical settings $S \gg P$ and therefore the relevant range for the inverse Lewis numbers is $L^{-1} \gg 1$.

The base state whose stability will be studied here is given by

$$\mathbf{v}_0 = \mathbf{0}, \quad T_0 = -z + \frac{1+B}{B}, \quad C_0 = \chi z + \text{const}, \quad p_0 = \text{const}. \tag{9}$$

III. LINEAR STABILITY ANALYSIS

We now study the stability of the base state given by Eq. (9) of the two-dimensional system in the plane (x,z) with respect to infinitesimal disturbances in the same plane. In this section $\boldsymbol{\nabla} = (\partial_x, \partial_z)$.

Linearization of Eqs. (7) around the base state, Eq. (9) results in

$$\boldsymbol{\nabla} \cdot \mathbf{v} = 0, \tag{10a}$$

$$\mathbf{v}_t = -\boldsymbol{\nabla} p + \nabla^2 \mathbf{v}, \tag{10b}$$

$$PT_t - w = \nabla^2 T, \tag{10c}$$

$$SC_t + L^{-1}\chi w = \nabla^2 C + \chi \nabla^2 T, \tag{10d}$$

where w is the z component of the fluid velocity field $\mathbf{v}$.

The boundary conditions, Eqs. (2) and (3), are rewritten as

$$\mathbf{v} = 0, \quad T_z = 0, \quad C_z = 0 \quad \text{at} \quad z = 0, \tag{10e}$$

$$w = 0, \quad T_z + BT = 0, \quad C_z - \chi BT = 0,$$

$$\partial_z \mathbf{u} + M \boldsymbol{\nabla}(T - C) = \mathbf{0} \quad \text{at} \quad z = 1. \tag{10f}$$

Introducing normal perturbations in the form

$$(\mathbf{v}, p, T, C) = \exp(ikx + \omega t)(\tilde{\mathbf{v}}, \tilde{p}, \tilde{T}, \tilde{C}) \tag{11}$$

into Eqs. (10) with ω being the growth rate of the perturbation with the wave number k and using the streamfunction $\tilde{\psi}$ to express the components of the two-dimensional flow field $\tilde{\mathbf{v}}$ results in

$$\tilde{\psi}'''' - 2k^2 \tilde{\psi}'' + k^4 \tilde{\psi} = \omega(\tilde{\psi}'' - k^2 \tilde{\psi}), \tag{12a}$$

$$\tilde{T}'' - k^2 \tilde{T} = \omega P \tilde{T} + ik\tilde{\psi}, \tag{12b}$$

$$\tilde{C}'' - k^2 \tilde{C} + \chi(\tilde{T}'' - k^2 \tilde{T}) = \omega S \tilde{C} - ik\chi L^{-1}\tilde{\psi}, \tag{12c}$$

$$\tilde{\psi} = 0, \quad \tilde{\psi}' = 0, \quad \tilde{T}' = 0, \quad \tilde{C}' = 0 \quad \text{at} \quad z = 0, \tag{12d}$$

$$\tilde{\psi} = 0, \quad \tilde{T}' + B\tilde{T} = 0, \quad \tilde{C}' - \chi B\tilde{T} = 0,$$

$$\tilde{\psi}'' + ikM(\tilde{T} - \tilde{C}) = 0 \quad \text{at} \quad z = 1, \tag{12e}$$

where prime denotes derivative with respect to z.

We study here the case of the long-wavelength instability of the system with poorly conducting boundaries. According to this we introduce the scaling

$$k = \epsilon K, \quad \omega = \epsilon^2 \overline{\omega}, \quad B = \epsilon^4 \beta, \quad \tilde{\psi} = \epsilon \tilde{\Psi}, \tag{13}$$

where ϵ is a small parameter serving therefore as a measure of supercriticality. The Marangoni number is expanded near the stability threshold as

$$M = M_0 + M_2 \epsilon^2 + M_4 \epsilon^4 + \cdots. \tag{14}$$

The dependent variables and the growth rate are also expanded into series of powers of ϵ:

$$(\tilde{\Psi}, \tilde{T}, \tilde{C}) = (\Psi_0, T_0, C_0) + \epsilon^2(\Psi_2, T_2, C_2) + \epsilon^4(\Psi_4, T_4, C_4) + \cdots, \tag{15}$$

$$\overline{\omega} = \omega_0 + \epsilon^2 \omega_2 + \epsilon^4 \omega_4 + \cdots. \tag{16}$$

The details of the following derivation are presented in Appendix A.

The dependence of the growth rate on the Marangoni number arising from the zero value of the characteristic determinant, see Appendix A, is determined by the quadratic equation

$$PS\Lambda_0^2+[P+S-S(\chi+1)m_0]\Lambda_0+1-(1+\chi+\chi L^{-1})m_0=0, \tag{17}$$

where Λ_0 is the rescaled growth rate of the disturbance defined as $\Lambda_0=\omega_0 K^{-2}$ and $m_0=M_0/48$. The explicit expression for $\Lambda_0(m_0)$ reads

$$\Lambda_0=\frac{S(\chi+1)m_0-(P+S)\pm\sqrt{S^2(\chi+1)^2m_0^2-2S[S(1-\chi)-P(1+\chi)]m_0+(S-P)^2}}{2PS}. \tag{18}$$

Equation (18) determines two instability modes, the monotonic one and the oscillatory one, that will be next considered separately.

A. Monotonic instability mode

Substituting $\Lambda_0=0$ into Eq. (17), we find that the monotonic instability boundary is determined by the relation

$$M_0=48[1+\chi(1+L^{-1})]^{-1}. \tag{19}$$

The critical value of the Marangoni number M_0 is positive if $\chi>\chi_1$,

$$\chi_1=-\frac{1}{1+L^{-1}}, \tag{20}$$

and negative if $\chi<\chi_1$. Recall that in the case of the standard thermocapillary effect ($\sigma_t=-\partial\sigma/\partial T^*>0$) the positive (negative) Marangoni number corresponds to heating (cooling) from below. In this paper we will consider only the case of positive Marangoni numbers.

Differentiating Eq. (17) with respect to M_0, we find that at the critical Marangoni number

$$\frac{d\Lambda_0}{dM_0}=\frac{[1+\chi(1+L^{-1})]^2}{48P[1+\chi(1+L^{-1}+L^{-2})]}. \tag{21}$$

Thus, we find that $d\Lambda_0/dM_0$ is positive if $\chi>\chi_2$,

$$\chi_2=-\frac{1}{1+L^{-1}+L^{-2}}, \tag{22}$$

and negative if $\chi<\chi_2$. Note that $\chi_1<\chi_2<0$ for any (positive) values of L.

We come to the conclusion that in the case $\chi>\chi_2$ both M_0 and $d\Lambda_0/dM_0$ are positive. This means that the growth rate is negative for M below the critical value M_0 and positive above the critical value, i.e., the boundary $M=M_0$ is indeed the threshold of the monotonic instability of the equilibrium state.

If the parameter χ lies in the interval $\chi_1<\chi<\chi_2$, then $M_0>0$ but $d\Lambda_0/dM_0<0$. It follows thus that M_0 is actually the boundary of *stabilization* of the monotonic mode which is unstable *below* that boundary and stable *above* it. We shall see in the following that in the case $\chi<\chi_2$ an oscillatory instability appears with the threshold lower than that given by Eq. (19).

If $\chi<\chi_1$, the instability appears for negative values of M. Because $d\Lambda_0/dM_0<0$, it is developed in the supercritical region, $M<M_0<0$.

Equation (A12) yields the expression for the growth rate ω_2,

$$\omega_2=\left[-\beta(1+\chi)+\frac{M_2}{48}K^{-2}m_0^{-2}-\frac{1}{15}m_0^{-1}K^4\right]\times[P(1+\chi)+S\chi(1+L^{-1})]^{-1}, \tag{23}$$

where $m_0=M_0/48$. Equation (23) can be rewritten in the form

$$\omega_2=\frac{\left\{-B(1+\chi)+\frac{M-M_0}{48}k^2[1+\chi(1+L^{-1})]^2-\frac{1}{15}k^4P[1+\chi(1+L^{-1})]\right\}}{\epsilon^4P[1+\chi(1+L^{-1}+L^{-2})]}. \tag{24}$$

It follows from Eq. (24) that the growth rate $\overline{\omega}$ has a local minimum at $k=0$ and its value there is negative, i.e., the instability is long-wavelength, when the denominator in Eq. (24) is positive and the B term in the numerator is negative. Thus, the condition for the long-wavelength instability to be monotonic is $\chi>\chi_2$.

B. Oscillatory instability mode

The oscillatory instability boundary is determined by the relation $\Lambda_0=\pm i\Omega_0$, where the oscillation frequency Ω_0 is real. Using the dispersion relation (17), we find that oscillatory instability appears in the region $-1<\chi<\chi_2$ at

$$M_0=\frac{48(1+L^{-1})}{L^{-1}(1+\chi)}, \tag{25}$$

with the frequency

$$\Omega_0=\frac{1}{S}\sqrt{-\frac{1+\chi(1+L^{-1}+L^{-2})}{1+\chi}}. \tag{26}$$

Details of the derivation in the case at hand are given in Appendix B.

As in the case of the monotonic instability, the solvability condition at fourth order of approximation determines the correction ω_2 to the eigenvalue. We present here only the expression for the real part of the coefficient ω_2 which determines the growth rate of the oscillatory instability

$$\mathrm{Re}[\omega_2]=-\frac{\beta}{2P}+\frac{(1+\chi)K^2M_2}{96P}+\frac{K^4m_0F(\chi)}{120P^2S}, \tag{27}$$

where $m_0=M_0/48$ and

$$F(\chi)=\chi[2(S^2-SP+P^2)-3(S+P)]+P(-4S+2P-3). \tag{28}$$

In order to ensure that short-wavelength disturbances decay, one has to require that $F(\chi)<0$. Recall that the oscillatory instability exists in the interval $-1<\chi<\chi_2$, where χ_2 is determined by Eq. (22). The function $F(\chi)$ varies linearly between the values that it takes at the ends of this interval, namely,

$$F(-1)=S(-2S-2P+3)$$

and

$$F(\chi_2)=-\frac{S^2P(4S+4P+3)}{S^2+SP+P^2}<0. \tag{29}$$

Thus, the oscillatory instability is long-wavelength in the whole interval of its existence, if $S>3/2-P$, which makes $F(-1)$ negative. The Schmidt number S is positive and typically large, and this condition is therefore satisfied.

It is important to emphasize that the frequency of oscillations ω_0 at the onset of instability is $O(\epsilon^2)$, while the characteristic growth rate of oscillations $\mathrm{Re}(\omega_2)$ is $O(\epsilon^4)$. This result will be employed in the nonlinear stability analysis of the oscillatory instability, see Sec. VI.

Figure 1 summarizes the results of linear stability analysis. It displays the neutral curves for both long-wavelength monotonic and oscillatory instabilities for $L^{-1}=20,100$, and 1000. For a fixed value of L^{-1} long-wavelength monotonic instability sets in for $\chi>\chi_2$. In the particular case of a pure liquid corresponding to $\chi=0$ the instability [30] is known to be monotonic with the critical Marangoni number $M_0=48$. At $\chi=\chi_2$ the long-wavelength oscillatory branch bifurcates off the monotonic one and manifests the instability threshold when $-1<\chi<\chi_2$. This long-wavelength oscillatory instability disappears when $\chi\leqslant-1$. The bifurcation structure remains the same for any $L^{-1}\gg1$. The critical Marangoni number for the oscillatory mode decreases with L^{-1} reaching a limiting curve $M_0=48(1+\chi)^{-1}$ in the limit of $L^{-1}\to\infty$. On the other hand, the critical Marangoni number for the monotonic mode increases with L^{-1} when $\chi<0$ and decreases when $\chi>0$.

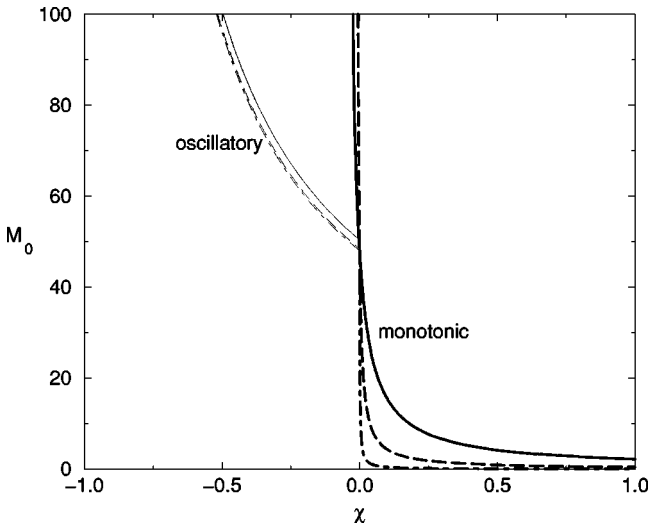

FIG. 1. Neutral curves for both long-wavelength monotonic and oscillatory instabilities and for various values of the inverse Lewis number L^{-1}. The thick and thin curves correspond to the monotonic and oscillatory modes, respectively. The solid, long-dashed, and dot-dashed lines correspond to $L^{-1}=20,100$, and 1000, respectively.

IV. LONG-WAVELENGTH NONLINEAR ANALYSIS FOR MONOTONIC INSTABILITY

In this section we study the nonlinear evolution of the three-dimensional system in the regime where the instability is long-wavelength. We use the technique of asymptotic expansions to derive a set of nonlinear evolution equations describing the spatiotemporal dynamics of the system.

The set of dimensionless governing equations and boundary conditions, Eqs. (7), is given by

$$\mathbf{u}_t+P^{-1}[(\mathbf{u}\cdot\boldsymbol{\nabla})\mathbf{u}+w\mathbf{u}_z]=-\boldsymbol{\nabla}p+\nabla^2\mathbf{u}+\mathbf{u}_{zz}, \tag{30a}$$

$$w_t+P^{-1}[(\mathbf{u}\cdot\boldsymbol{\nabla})w+ww_z]=-p_z+\nabla^2w+w_{zz}, \tag{30b}$$

$$\boldsymbol{\nabla}\cdot\mathbf{u}+w_z=0, \tag{30c}$$

$$P\Theta_t+\mathbf{u}\cdot\boldsymbol{\nabla}\Theta+w\Theta_z-w=\nabla^2\Theta+\Theta_{zz}, \tag{30d}$$

$$S\Sigma_t+L^{-1}(\mathbf{u}\cdot\boldsymbol{\nabla}\Sigma+w\Sigma_z+\chi w)=\nabla^2\Sigma+\Sigma_{zz}+\chi(\nabla^2\Theta+\Theta_{zz}), \tag{30e}$$

$$\mathbf{u}=w=\Theta_z=\Sigma_z=0 \quad \text{at} \quad z=0, \tag{30f}$$

$$w=\Sigma_z-\chi B\Theta=0, \quad \Theta_z+B\Theta=0,$$

$$\partial_z\mathbf{u}+M\boldsymbol{\nabla}(\Theta-\Sigma)=\mathbf{0} \quad \text{at} \quad z=1. \tag{30g}$$

The functions $\Theta(x,y,z,t)$ and $\Sigma(x,y,z,t)$ constitute the deviations of temperature and concentration from their respective equilibrium values, Eq. (9), and vector $\mathbf{u}$ is a two-dimensional projection of $\mathbf{v}$ onto the x-y plane. Here subscripts denote the derivatives with respect to the corresponding variables, $\boldsymbol{\nabla} \equiv (\partial_x, \partial_y)$, $\nabla^2 = \partial_x^2 + \partial_y^2$, and $\nabla^4 = (\nabla^2)^2$.

The Marangoni number near the critical point is represented in the form

$$M = M_0 + M_2 \epsilon^2 + M_4 \epsilon^4 + \cdots, \tag{31}$$

where M_0 is the value of the Marangoni number at the threshold of instability, and ϵ is a small parameter serving therefore as a measure of supercriticality.

Introduce the rescaled spatial and temporal variables by

$$X = \epsilon x, \quad Y = \epsilon y, \quad Z = z, \quad \tau = \epsilon^4 t. \tag{32a}$$

The Biot number B is assumed to be small,

$$B = \epsilon^4 \beta. \tag{32b}$$

The appropriate scaling for the fluid velocity and pressure fields $\{\mathbf{u}, w, p\}$ is chosen as

$$\mathbf{u} = \epsilon \mathbf{U}, \quad w = \epsilon^2 W, \quad p = \Pi. \tag{32c}$$

The dependent variables are represented as the series in powers of ϵ,

$$\begin{pmatrix} \mathbf{U} \\ W \\ \Theta \\ \Sigma \end{pmatrix} = \begin{pmatrix} \mathbf{U}^{(0)} \\ W^{(0)} \\ \Theta^{(0)} \\ \Sigma^{(0)} \end{pmatrix} + \epsilon^2 \begin{pmatrix} \mathbf{U}^{(2)} \\ W^{(2)} \\ \Theta^{(2)} \\ \Sigma^{(2)} \end{pmatrix} + \epsilon^4 \begin{pmatrix} \mathbf{U}^{(4)} \\ W^{(4)} \\ \Theta^{(4)} \\ \Sigma^{(4)} \end{pmatrix} + \cdots. \tag{33}$$

The details of the derivation are given in Appendix C.

The solution of the problem at zeroth order is

$$\Theta^{(0)} = F(X,Y,\tau), \quad \Sigma^{(0)} = G(X,Y,\tau), \tag{34}$$

$$\mathbf{U}^{(0)} = 12 m_0 Z(2-3Z) \boldsymbol{\nabla}(F-G), \tag{35a}$$

$$W^{(0)} = 12 m_0 Z^2 (Z-1) \nabla^2 (F-G), \tag{35b}$$

$$\Pi^{(0)} = \Pi^{(0)}(x,y,\tau) = -72 m_0 (F-G), \tag{36}$$

where $m_0 = M_0/48$ and F and G are functions yet unknown to be determined later.

The solvability condition gives the critical value of the Marangoni number

$$M_0 = 48[1 + \chi(1 + L^{-1})]^{-1}$$

thus

$$m_0 = [1 + \chi(1 + L^{-1})]^{-1}. \tag{37}$$

It follows from the solvability condition at second order that functions F and G are related to each other via

$$G = -\chi(1 + L^{-1})[F - \langle\langle F \rangle\rangle], \tag{38}$$

where $\langle\langle F \rangle\rangle = \mathcal{L}^{-1} \int\int F(X,Y,\tau) dX dY$, and the integration is carried out over the domain of periodicity in the X-Y plane of the area $\mathcal{L}$. The relationship (38) shows that the average temperature disturbance per unit area $\langle\langle F \rangle\rangle$ may change in time due to imperfect insulation of the boundaries, however, the average concentration disturbance per unit area $\langle\langle G \rangle\rangle = \mathcal{L}^{-1} \int\int G(X,Y,\tau) dX dY$ does not change in time in the absence of solute sources.

Applying the solvability condition at second order yields the set of evolution equations in terms of the functions $T^{(0)} = F(X,Y,\tau)$ and $E(X,Y,\tau)$, when the latter has the meaning of the mean-flow stream function (for details, see Appendix C):

$$\begin{aligned} &\alpha P F_\tau + \beta(1+\chi)F + \gamma_1 \nabla^2 F + \gamma_2 \nabla^4 F + \gamma_3 \boldsymbol{\nabla} \cdot (\boldsymbol{\nabla} F \nabla^2 F) \\ &\quad + \gamma_4 \nabla^2 (|\boldsymbol{\nabla} F|^2) - \gamma_5 \boldsymbol{\nabla} \cdot [\boldsymbol{\nabla} F |\boldsymbol{\nabla} F|^2] \\ &\quad + \gamma_6 (\partial_X F \partial_Y E - \partial_Y F \partial_X E) \\ &= P \chi L^{-1} (1 + L^{-1}) \partial_\tau (\langle\langle F \rangle\rangle), \end{aligned} \tag{39a}$$

$$\nabla^2 E = -\frac{936}{35P} (\partial_Y F \nabla^2 \partial_X F - \partial_X F \nabla^2 \partial_Y F), \tag{39b}$$

where

$$\alpha = 1 + \chi(1 + L^{-1} + L^{-2}), \quad \gamma_1 = \tfrac{1}{48} M_2 (1 + \chi + \chi L^{-1})^2,$$

$$\gamma_2 = \tfrac{1}{15}(1 + \chi + \chi L^{-1}),$$

$$\gamma_3 = \frac{1 + \chi + \chi L^{-1}}{5P} + \frac{1 + \chi(1 + L^{-1} + L^{-2})}{10},$$

$$\gamma_4 = \frac{1 + \chi + \chi L^{-1}}{10P} + \frac{3[1 + \chi(1 + L^{-1} + L^{-2})]}{5},$$

$$\gamma_5 = \tfrac{48}{35}[1 + \chi(1 + L^{-1})(1 + L^{-2})],$$

$$\gamma_6 = -\tfrac{1}{3}[1 + \chi(1 + L^{-1} + L^{-2})]. \tag{39c}$$

Equations (39) will provide us with the details of the weakly nonlinear dynamics of the system when the instability is monotonic. Note that Eqs. (39a) and (39b) are similar to those derived in Ref. [25] in the case of long-wavelength Marangoni instability in a pure liquid when the term $\langle\langle F \rangle\rangle$ vanishes.

As it is known from the simulation of the long-wavelength Marangoni convection in a pure liquid, the mean flow is of minor importance in the case of regular patterns, but it is crucial for the dynamics of defects and for the development of a spatiotemporal chaos [31]. In the case of a two-dimensional layer lying in the X-Z plane Eqs. (39) reduce to the single evolution equation

$$\alpha P F_\tau + \beta(1+\chi)F + \gamma_1 \partial_X^2 F + \gamma_2 \partial_X^4 F + (\tfrac{1}{2}\gamma_3 + \gamma_4)\partial_X^2[(\partial_X F)^2] - \tfrac{1}{3}\gamma_5 \partial_X[(\partial_X F)^3] = P\chi L^{-1}(1+L^{-1})\ \partial_\tau(\langle\langle F\rangle\rangle). \quad (40)$$

It is important to emphasize that the dispersion relation giving the relationship between the linear growth rate of the disturbance and its dimensionless wave number, as obtained from Eq. (40), is identical to that given in Eq. (24).

In the limit of large Prandtl number, $P \gg 1$, Eqs. (39) reduce so that both the γ_6 term in Eqs. (39a) and (39b) vanish. Under the transformation

$$\tau = c_1 \tau_1, \quad F = c_2 \mathcal{F}, \quad (X,Y) = c_3(\xi,\eta),$$

with

$$c_1 = \frac{4\alpha P \gamma_2}{\gamma_1}, \qquad c_2 = \left(\frac{\gamma_5}{\gamma_2}\right)^{1/2}, \quad c_3 = \left(\frac{2\gamma_2}{\gamma_1}\right)^{1/2},$$

Eq. (39a) is rewritten in the form

$$\mathcal{F}_{\tau_1} + b\mathcal{F} + 2\nabla_1^2 \mathcal{F} + \nabla_1^4 \mathcal{F} - \boldsymbol{\nabla}_1 \cdot (\boldsymbol{\nabla}_1 \mathcal{F} |\boldsymbol{\nabla}_1 \mathcal{F}|^2) + s_1 \boldsymbol{\nabla}_1 \cdot (\boldsymbol{\nabla}_1 \mathcal{F} \nabla_1^2 \mathcal{F}) + s_2 \nabla_1^2 (|\boldsymbol{\nabla}_1 \mathcal{F}|^2) = \chi L^{-1}(1+L^{-1})\alpha^{-1}\ \partial_{\tau_1}(\langle\langle \mathcal{F}\rangle\rangle), \quad (41a)$$

where

$$s_1 = \frac{\gamma_3 c_3^{-4} c_1 c_2}{\alpha P}, \quad s_2 = \frac{\gamma_4 c_3^{-4} c_1 c_2}{\alpha P}, \quad b = \frac{\beta(1+\chi)c_1}{\alpha P}, \quad (41b)$$

and $\boldsymbol{\nabla}_1 \equiv (\partial_\xi, \partial_\eta)$, $\nabla_1^2 = \partial_\xi^2 + \partial_\eta^2$, $\nabla_1^4 = (\nabla_1^2)^2$. Note that Eq. (41a) is similar to that derived by Knobloch [24] for the case of long-wavelength Marangoni instability in a pure liquid for infinite Prandtl number and for large times, so that the right-hand side term there vanishes.

In what follows we will enforce periodic boundary conditions for $F(X,Y,\tau)$ in the X-Y plane. Integrating Eq. (39a) over the domain of periodicity yields

$$\alpha P \partial_\tau(\langle\langle F\rangle\rangle) + \beta(1+\chi)\langle\langle F\rangle\rangle = P\chi L^{-1}(1+L^{-1})\partial_\tau(\langle\langle F\rangle\rangle), \quad (42)$$

which reduces to

$$\partial_\tau(\langle\langle F\rangle\rangle) = -\beta P^{-1}\langle\langle F\rangle\rangle. \quad (43)$$

Thus, $\langle\langle F\rangle\rangle = \text{const} \times \exp(-\beta P^{-1}\tau)$ and $\langle\langle F\rangle\rangle$ vanishes in the limit of large times.

V. BIFURCATION ANALYSIS

In this section we derive nonlinear amplitude equations for patterns of three kinds, namely, rolls, squares, and hexagons, and study their stability in the case of large Prandtl number. To achieve this goal we notice from Eq. (41a) that the critical value of the rescaled Biot number is $b=1$, while the critical wave number is $k=1$. We consider here the dynamics of the system at large times, therefore the right-hand side term in Eq. (41a) vanishes.

A. Rolls versus squares

We denote as δ a small parameter being a measure of the distance between the critical and actual values of the Biot number $b = 1-\delta^2$, scale time as $\overline{\tau} = \delta^2 \tau_1$, and seek for a solution of Eq. (41a) in the form of series in powers of δ, $\mathcal{F} = \delta \mathcal{F}_1 + \delta^2 \mathcal{F}_2 + \delta^3 \mathcal{F}_3 + \cdots$. Substituting these into Eq. (41a) one obtains at first order in δ,

$$\nabla_1^4 \mathcal{F}_1 + 2\nabla_1^2 \mathcal{F}_1 + \mathcal{F}_1 = 0. \quad (44)$$

The solution for Eq. (44) is now chosen as

$$\mathcal{F}_1 = A_1(\overline{\tau})\cos\xi + B_1(\overline{\tau})\cos\eta, \quad (45)$$

where $A_1(\overline{\tau})$ and $B_1(\overline{\tau})$ are real amplitude functions of the planform. Note that the planform is a roll when either $B_1 = 0, A_1 \neq 0$ or $A_1 = 0, B_1 \neq 0$. The planform is square when $B_1 = A_1$.

Elimination of secular terms in the problem at third order in δ yields a set of the amplitude equations in the form

$$\frac{dA_1}{d\overline{\tau}} = A_1 - \Gamma_1 A_1^3 - \Gamma_2 A_1 B_1^2,$$

$$\frac{dB_1}{d\overline{\tau}} = B_1 - \Gamma_1 B_1^3 - \Gamma_2 B_1 A_1^2, \quad (46)$$

where

$$\Gamma_1 = \tfrac{1}{36}[27 + 4(s_1+2s_2)^2] > 0, \quad \Gamma_2 = \tfrac{1}{2}(1 - 2s_1^2 + 4s_1 s_2). \quad (47)$$

In the particular case of the roll pattern in the ξ direction, $A_1 \neq 0, B_1 = 0$ the set of amplitude equations, Eq. (46), reduces to a single equation

$$\frac{dA_1}{d\overline{\tau}} = A_1 - \Gamma_1 A_1^3. \quad (48)$$

A similar equation is obtained in terms of B_1 for the rolls in the η direction. As the coefficient of the cubic term of Eq. (48) is positive for all values of the Soret number χ and the inverse Lewis number L^{-1}, roll patterns bifurcate supercritically. The amplitude of the corresponding steady roll pattern is obtained by $A_1 = 1/\sqrt{3 + 4(s_1+2s_2)^2/9}$.

In the particular case of the square pattern, $A_1 = B_1$, the amplitude equation obtained from the reduction of Eqs. (46) is

$$\frac{dA_1}{d\overline{\tau}} = A_1 - (\Gamma_1 + \Gamma_2)A_1^3, \quad (49)$$

where

$$\Gamma_1+\Gamma_2=\tfrac{1}{36}[45-32s_1^2+88s_1s_2+16s_2^2]. \tag{50}$$

Substituting s_1 and s_2 from Eq. (41b) into Eq. (50) and taking the limit of large inverse Lewis number L^{-1}, Eq. (50), yields

$$\Gamma_1+\Gamma_2=\frac{1}{25P^2}[16+\chi^2L^{-2}+302P\chi^2L^{-3} + P^2(1125+268\chi^2L^{-4})], \tag{51}$$

which is positive. Thus, in the limit of large L^{-1} square patterns bifurcate supercritically, and the amplitude of the emerging pattern is $A_1=B_1=(\Gamma_1+\Gamma_2)^{-1/2}$.

We now turn to the study of stability of both roll and square patterns. The fixed points of the dynamical system [Eqs. (46)] $(A_1=\pm\Gamma_1^{-1/2},B_1=0)$ and $(A_1=0,B_1=\pm\Gamma_1^{-1/2})$ represent roll patterns, while $[A_1=B_1=\pm(\Gamma_1+\Gamma_2)^{-1/2}]$ represents a square pattern.

Linear stability analysis of both the roll patterns reveals that they can be stable only when $0<\Gamma_1<1$. However, in the relevant limit of large inverse Lewis numbers L^{-1},

$$1-\Gamma_1=-\tfrac{169}{448}M_2^2\chi^4L^{-8}+O(L^{-7})<0, \tag{52}$$

which implies that the roll patterns are unstable.

Stability analysis of the square pattern shows that one of the eigenvalues of the stability matrix is always negative, while the other is negative when $\Gamma_2<\Gamma_1$. In the physically relevant limit of $L^{-1}\gg 1$,

$$\Gamma_2-\Gamma_1=\tfrac{45}{8}M_2^2\chi^4L^{-8}+O(L^{-7})<0. \tag{53}$$

Thus, the square pattern is stable in the limit of large L^{-1}. This result obtained for the case of binary liquids matches that obtained for pure liquids in the case of small Biot numbers.

B. Hexagons

Let us now choose a different definition of δ by $b=1-\delta$ and a different scaling of time according to $\bar{\tau}=|\delta|\tau_1$, while the sought form of the solution remains the same as in Sec. V A.

We now follow the analysis presented by Shtilman and Sivashinsky [25] for stability of hexagonal patterns obtained as a solution of Eq. (44) at first order of expansion in δ,

$$\mathcal{F}_1=A_1(\bar{\tau})\left(\cos\xi+2\cos\frac{\xi}{2}\cos\frac{\sqrt{3}\eta}{2}\right), \tag{54}$$

where $A_1(\bar{\tau})$ is a real function of time $\bar{\tau}$, yet unknown.

Elimination of secular terms in the problem at third order in δ yields

$$\frac{dA_1}{d\bar{\tau}}=A_1+2\lambda_2A_1A_2-\lambda_3A_1^3, \tag{55}$$

where

$$\lambda_2=\frac{s_2-s_1}{2},\quad \lambda_3=\frac{9}{4}+\frac{s_2(97s_1+113s_2)}{72}+\frac{s_1(s_1+2s_2)}{9}, \tag{56}$$

and $A_2(\bar{\tau})$ is a real amplitude of the general solution of Eq. (44) at second order in δ.

Defining a function $A(\bar{\tau})$ via $A=A_1+\delta A_2$ one can combine Eq. (55) with the solvability condition at second order in δ to obtain

$$\frac{dA}{d\bar{\tau}}=\mathrm{sgn}(\delta)A+\lambda_2A^2-\delta\lambda_3A^3, \tag{57}$$

being accurate to $o(\delta^2)$.

Turning back to the values of time τ_1 and $a=\delta A$ being the amplitude of the hexagonal pattern one obtains the amplitude equation in the form

$$\frac{da}{d\tau_1}=\delta a+\lambda_2a^2-\lambda_3a^3. \tag{58}$$

It is found that in the limit of $L^{-1}\gg 1$ the coefficient λ_3 is positive.

It follows from Eq. (58) that the amplitude a_s of steady hexagonal patterns satisfies the relationship

$$\delta=\lambda_3a_s^2-\lambda_2a_s. \tag{59}$$

Thus two possible steady hexagonal patterns can emerge for

$$\delta\geqslant\Delta\equiv-\frac{\lambda_2^2}{4\lambda_3}. \tag{60}$$

In the limit of large inverse Lewis numbers L^{-1} one obtains

$$\Delta=-\frac{225}{9508}+\frac{1\,070\,685}{45\,201\,032}\frac{L}{P}+O(L^2). \tag{61}$$

The stability analysis in the framework of the amplitude equation (58) shows that in the subcritical region $\delta<0$ one of the solutions a_s for Eq. (59) is linearly stable, as well as the trivial solution $a=0$ corresponding to the quiescent state, while the other solution of Eq. (59) is unstable. In the supercritical region $\delta>0$ both of the solutions, a_s, are stable, while the solution $a=0$ is unstable. Note, however, that the ansatz (54) and the amplitude equation (58) ignore the phase disturbances that make one of the solutions a_s unstable. For a general discussion on stability of hexagonal patterns the reader is referred to Ref. [32].

We conclude with the study of the flow direction in the stable hexagonal patterns we have investigated here. According to Eq. (54), the sign of $\mathcal{F}_1$ in the center of the hexagon positioned around $\xi=\eta=0$ coincides with the sign of A_1, while the stable branch of the hexagons amplitude, if the phase disturbances are taken into account, has $A_1>0$ when $\lambda_2>0$ and $A_1<0$ when $\lambda_2<0$. As follows from Eqs. (56) and (41b) $\lambda_2=(\gamma_4-\gamma_3)c_3^{-4}c_1c_2/(2\alpha P)$, and therefore the sign of λ_2 coincides with that of $\gamma_4-\gamma_3=-(1+\chi+\chi L^{-1})/10P+[1+\chi(1+L^{-1}+L^{-2})]/2$. In the domain of

monotonic instability, $\chi>\chi_1=-1/(1+L^{-1}+L^{-2})$, $1+\chi(1+L^{-1}+L^{-2})>0$, and $1+\chi+\chi L^{-1}=[1+\chi(1+L^{-1}+L^{-2})]-\chi L^{-2}>0$.

Thus, we can conclude that the sign of $\gamma_4-\gamma_3$ depends on P. If $P<P_*, P_*=0.2(1+\chi+\chi L^{-1})/[1+\chi(1+L^{-1}+L^{-2})]$, then $\lambda_2<0$, a cold spot emerges in the center of the hexagonal cell, and the flow is directed downwards. If $P>P_*$, a hot spot emerges in the center of the hexagonal cell, and the flow is directed upwards. Because in the physically relevant case of $L^{-1}\gg 1$, $P_*\approx 0.2L\ll 1$, and therefore $W(\xi=0,\eta=0)>0$ for practically any P. In the opposite (unphysical) limit of $L\gg 1$ we reproduce the result $P_*=0.2$ known in the case of a pure liquid.

VI. LONG-WAVELENGTH NONLINEAR ANALYSIS FOR OSCILLATORY INSTABILITY

A. Derivation of amplitude equations

The present section is devoted to the derivation of the amplitude equations governing the oscillatory instability. We shall restrict ourselves to the consideration of two-dimensional flows in the x-z plane. Using the streamfunction ψ and eliminating the pressure, we rewrite the system of equations (30) in the form

$$\nabla^2\psi_t+P^{-1}[\psi_z\nabla^2\psi_x-\psi_x\nabla^2\psi_z]=\nabla^4\psi, \tag{62a}$$

$$P\Theta_t+\psi_z\Theta_x-\psi_x\Theta_z+\psi_x=\nabla^2\Theta, \tag{62b}$$

$$S\Sigma_t+L^{-1}(\psi_z\Sigma_x-\psi_x\Sigma_z-\chi\psi_x)=\nabla^2\Sigma+\chi\nabla^2\Theta, \tag{62c}$$

$$\psi=\psi_z=\Theta_z=\Sigma_z=0 \quad \text{at} \quad z=0, \tag{62d}$$

$$\psi=\Sigma_z-\chi B\Theta=0, \quad \Theta_z+B\Theta=0,$$

$$\psi_{zz}+M(\Theta_x-\Sigma_x)=0 \quad \text{at} \quad z=1. \tag{62e}$$

In this section $\nabla^2=\partial_x^2+\partial_z^2$.

According to the results of the linear theory, in the limit of small Biot numbers, Eq. (32b), the oscillatory instability takes place near the threshold in a narrow interval of small wave numbers. Similar to the case of the monotonic instability, we expand the Marangoni number in the form of Eq. (31) and introduce the rescaled spatial variables

$$X=\epsilon x, \quad Z=z. \tag{63}$$

In contradistinction to the case of the monotonic instability, where it was sufficient to use only one ''slow'' time scale, $\tau=\epsilon^4 t$, the description of the oscillatory instability should be based on the consideration of two slow time scales,

$$T=\epsilon^2 t, \quad \tau=\epsilon^4 t. \tag{64}$$

Indeed, it was shown in Sec. III that the frequency of oscillations is $O(\epsilon^2)$, while the characteristic growth rate of oscillations is $O(\epsilon^4)$. The streamfunction is rescaled as

$$\psi=\epsilon\Psi. \tag{65}$$

The details of the derivation are presented in Appendix D.

The solution of the equations at zeroth order is given by

$$\Theta^{(0)}=F(X,T,\tau), \quad \Sigma^{(0)}=G(X,T,\tau),$$

$$\Psi^{(0)}=12m_0(F_X-G_X)(Z^2-Z^3), \tag{66}$$

where F and G are amplitude functions, yet unknown, and $m_0=M_0/48$ is the rescaled value of the critical Marangoni number.

Substituting Eq. (25) for the leading-order threshold of the oscillatory instability, we can rewrite the solvability condition at second order as

$$F_T=\frac{L^{-1}\chi-1}{L^{-1}P(1+\chi)}F_{XX}+m_0P^{-1}G_{XX}, \tag{67}$$

$$G_T=\chi\frac{L^{-1}+2+\chi}{L^{-1}P(1+\chi)}F_{XX}-\frac{L^{-1}\chi-1}{L^{-1}P(1+\chi)}G_{XX}. \tag{68}$$

Substituting Eqs. (66) and the solution of the problem at second order into the solvability conditions at fourth order, we obtain the following amplitude equations:

$$\begin{aligned}Q_T+F_\tau=&\frac{1-m_0}{P}Q_{XX}+\frac{m_0}{P}R_{XX}-\frac{\beta}{P}F-\frac{M_2}{48P}(F_{XX}-G_{XX})-\frac{m_0^2}{20P}(13+4P^{-1}+12\chi)(F_X^2)_{XX}\\&+\frac{m_0^2}{10P}(7+4P^{-1}+6L^{-1}+6\chi)(F_XG_X)_{XX}-\frac{m_0^2}{20P}(1+4P^{-1}+12L^{-1})(G_X^2)_{XX}+\frac{48m_0^2}{35P}[F_X(F_X-G_X)^2]_X\\&+\frac{m_0}{20PS}[(S-\chi)F_{XXXX}-PG_{XXXX}]-\frac{m_0}{10P}\left[1-\frac{m_0(1+\chi)}{3}+\frac{m_0(1+\chi)}{2P}-\frac{m_0\chi}{3}L^{-1}\right](F_{XXXX}-G_{XXXX}),\end{aligned} \tag{69}$$

$$R_T+G_\tau=\chi\left(\frac{1}{S}+\frac{m_0}{P}\right)Q_{XX}+\left(\frac{1}{S}-\frac{m_0\chi}{P}\right)R_{XX}+\frac{M_2\chi}{48P}(F_{XX}-G_{XX})+\frac{\chi m_0^2}{20P}\left(1+\frac{4}{P}+13L^{-1}\right)(G_X^2)_{XX}$$
$$+\frac{m_0^2\chi}{20P}\left(13+L^{-1}+\frac{4}{P}+12\chi\right)(F_X^2)_{XX}-\frac{m_0^2\chi}{10P}\left(7+7L^{-1}+\frac{4}{P}+6\chi\right)(F_XG_X)_{XX}+\frac{48m_0^2}{35P}[F_XG_X\{(L^{-1}+2\chi)F_X$$
$$-(\chi+2L^{-1})G_X\}]_X+\frac{144m_0^2}{35P}(L^{-1}G_X^2G_{XX}-\chi F_X^2F_{XX})+\frac{m_0\chi}{20PS}[G_{XXXX}+(\chi-L^{-1})F_{XXXX}]$$
$$+\frac{m_0\chi}{10P}\left[1+\frac{m_0}{2P}(1+\chi)-\frac{m_0}{3}(1+\chi+\chi L^{-1})\right](F_{XXXX}-G_{XXXX}). \tag{70}$$

The solvability conditions for Q and R determine the evolution of the amplitudes F and G in the slow time scale τ.

Note that a similar approach was used by Cox [29] in the case of Rayleigh-Bénard convection.

B. Traveling and standing waves

The crucial issues that can be addressed by means of weakly nonlinear amplitude equations are the type of bifurcation (supercritical vs subcritical) and the stability of spatially periodic traveling and standing waves. These questions are considered in the present section.

The leading-order amplitude equations, which describe the oscillations on the time scale characterized by the variable T, are linear. Thus, any superposition of waves with arbitrary wave numbers satisfy these equations. We restrict ourselves to *spatially periodic* solutions

$$F(X,\tau,T)=F_1(\tau)e^{i(KX-\Omega_0K^2T)}+F_{-1}(\tau)e^{i(-KX-\Omega_0K^2T)}+\text{c.c.}, \tag{71}$$

$$G(X,\tau,T)=a_2[F_1(\tau)e^{i(KX-\Omega_0K^2T)}+F_{-1}(\tau)e^{i(-KX-\Omega_0K^2T)}]+\text{c.c.}, \tag{72}$$

where Ω_0 and a_2 are determined by Eqs. (26) and (B1), $2\pi/K$ is the spatial period of the wave, $F_1(\tau)$ and $F_{-1}(\tau)$ are amplitude functions, yet undetermined, and c.c. denotes complex conjugate.

Substituting Eqs. (71) and (72) into Eqs. (69) and (70), yields a nonhomogeneous linear system for functions Q and R. The corresponding solutions can be found in the form

$$Q=\sum_{m=-3}^{3}\sum_{n=-3}^{3}Q_{n,m}(\tau)e^{i(mKX-n\Omega_0K^2T)},$$

$$R=\sum_{m=-3}^{3}\sum_{n=-3}^{3}R_{n,m}(\tau)e^{i(mKX-n\Omega_0K^2T)}.$$

For the pairs $(Q_{1,1},R_{1,1})$ and $(Q_{-1,1},R_{-1,1})$ one obtains sets of linear algebraic equations with determinants equal to zero. The corresponding solvability conditions yield a set of nonlinear amplitude equations

$$\frac{dF_1}{d\tau}=(\omega_2-\kappa_1|F_1|^2-\kappa_2|F_{-1}|^2)F_1, \tag{73}$$

$$\frac{dF_{-1}}{d\tau}=(\omega_2-\kappa_1|F_{-1}|^2-\kappa_2|F_1|^2)F_{-1}, \tag{74}$$

where $\omega_2=\omega_{2r}+i\omega_{2i}$ is the linear complex growth rate [ω_{2r} determined by Eq. (27)], $\kappa_1=\kappa_{1r}+i\kappa_{1i}$ and $\kappa_2=\kappa_{2r}+i\kappa_{2i}$ are complex Landau constants. The real parts of the Landau constants κ_{1r} and κ_{2r} determine the type of bifurcation and govern the selection of a specified kind of waves, either traveling or standing one. Indeed, taking

$$F_1=r_1e^{i\theta_1},\quad F_{-1}=r_{-1}e^{i\theta_{-1}}, \tag{75}$$

where r_j, θ_j, $j=\pm1$, are real, and substituting Eq. (75) into Eqs. (73) and (74), one finds

$$\frac{dr_1}{d\tau}=(\omega_{2r}-\kappa_{1r}r_1^2-\kappa_{2r}r_{-1}^2)r_1, \tag{76}$$

$$\frac{dr_{-1}}{d\tau}=(\omega_{2r}-\kappa_{1r}r_{-1}^2-\kappa_{2r}r_1^2)r_{-1} \tag{77}$$

(equations for θ_j, $j=\pm1$, are irrelevant). A straightforward stability analysis shows that the standing wave solution $r_1=r_{-1}=\sqrt{\omega_{2r}/(\kappa_{1r}+\kappa_{2r})}$ is stable if $\kappa_{1r}+\kappa_{2r}>0$, $\kappa_{1r}>\kappa_{2r}$, while the traveling wave solutions $r_1=\sqrt{\omega_{2r}/\kappa_{1r}}$, $r_{-1}=0$, and $r_1=0$, $r_{-1}=\sqrt{\omega_{2r}/\kappa_{1r}}$ are stable if $\kappa_{2r}>\kappa_{1r}>0$.

The direct computation yields

$$\kappa_{1r}=\frac{24K^4L(1+L)}{35P(1+\chi)}P^2[-(1+\chi)+(3+2\chi^2)L^{-1}+\chi L^{-2}],$$

$$\kappa_{2r}=2\kappa_{1r}.$$

Recall that the oscillatory instability takes place when

$$\chi<\chi_2=-\frac{1}{1+L^{-1}+L^{-2}}<0.$$

In the relevant case of $L \ll 1$, we find that the bifurcation of traveling and standing wave solutions is supercritical only if χ belongs to the narrow interval

$$\chi_* < \chi < \chi_2, \quad \chi_* = -3L + O(L^2). \tag{78}$$

In the latter case, standing waves are unstable, thus the traveling waves are the selected kind of flow. Otherwise, a subcritical instability of the equilibrium state, which cannot be studied by means of a weakly nonlinear theory, takes place.

VII. DISCUSSION AND CONCLUSIONS

We now discuss the distinctions between the amplitude equations obtained for the Marangoni convection in a binary liquid and those obtained for a pure fluid.

The main specific feature of the Marangoni convection in a binary liquid is the existence of *three* slowly varying fields, namely, the fields of temperature F, concentration G, and the mean flow E. In the case of a pure liquid, only two fields, F and E, are present. A peculiarity of the concentration is its global conservation due to the absence of solute sources.

In the case of the monotonic instability, the fields F and G are directly related to each other by the expression given in Eq. (38). Therefore, the field G can be easily eliminated from the set of governing equations, and the latter are similar to those obtained for a pure fluid (see Refs. [25,26]), except for the additional *global-control* term on the right-hand side of Eq. (39a), which turns the amplitude equation into an integrodifferential one. However, this feature of the amplitude equations (39) does not affect the long-term dynamics of the system, because of the relation (43).

In the case of the oscillatory instability, the leading-order oscillations are characterized by a *time delay* determined by the *complex* parameter a_2 [see Eq. (B1)]. *Two-component* functions (F,G) and (Q,R) are used for the closed description of the system evolution. In the case of the Rayleigh-Bénard convection, such functions have been used by Cox [29]. Note, however, that the final Landau equations (73) and (74) are written in terms of the *scalar* amplitudes F_1 and F_{-1}, because the spatial Fourier components of the fields F and G are not independent. Similar amplitude equations were earlier derived in the context of the Rayleigh-Bénard convection by Pismen [28].

This paper presents linear and weakly nonlinear analyses and an investigation of pattern formation in long-wavelength Marangoni instability in a binary liquid layer open to the ambient gas phase with poorly conducting boundaries, when the Soret effect is taken into account. The liquid layer is assumed to be sufficiently thin and with sufficiently high surface tension, so that the mathematical model that neglects both buoyancy-driven convection and deformation of the liquid-gas interface is valid. Although most of the results are presented for general values of the dimensionless parameters of the problem, the physically relevant range of the inverse Lewis number is $L^{-1} \gg 1$.

Linear stability analysis reveals that both monotonic and oscillatory modes of instability exist here. It is found that monotonic instability sets in when the Soret number χ exceeds the value $\chi_2 = -(1 + L^{-1} + L^{-2})^{-1}$, $\chi > \chi_2$, and the critical value of the Marangoni number is $M_{0,mon} = 48[1 + \chi(1 + L^{-1})]^{-1}$. The oscillatory instability sets in when $-1 < \chi < \chi_2$ and the critical value of the Marangoni number is $M_{0,osc} = 48(1 + L)(1 + \chi)^{-1}$, while the frequency at the threshold is determined by Eq. (26). In the interval $\chi < \chi_1 = -(1 + L^{-1})^{-1}$ the monotonic mode is unstable when the value of the Marangoni number is below the critical value which is negative.

Long-wavelength nonlinear analysis of both monotonic and oscillatory instabilities yields sets of nonlinear evolution equations that govern the spatiotemporal dynamics of the system. In the case of monotonic instability, as in the case of a pure liquid, one of the two equations is of evolution type, while the other is elliptic and describe convective effects in the layer that vanish when the Prandtl number of the liquid is large. Bifurcation analysis based on the evolution equation for a binary liquid with large Prandtl number yields amplitude equations for roll, square and hexagon patterns. It is shown that roll patterns are found to be unstable, while square patterns are stable in the physically relevant limit of large L^{-1}. Hexagonal patterns are found to bifurcate transcritically, and a steady stable hexagonal pattern is possible. We expect that the hexagonal pattern appears in the subcritical region corresponding to Eq. (60), and it is replaced by the square pattern at a finite value of $M - M_0$. Because the stability analysis based on amplitude equations is not reliable for finite $M - M_0$, we postpone the elucidation of this question to the future strongly nonlinear analysis. In the case of oscillatory instability the set of nonlinear equations consists of two equations of evolution type. It is found that bifurcation of both standing and traveling waves is supercritical in the range $\chi_* < \chi < \chi_2$, where $\chi_* = -3L + O(L^2)$. In this range of the Soret number standing waves are found to be unstable, while traveling waves appear to be stable. Numerical study of the nonlinear evolution equations derived in this paper is not attempted here and will be the scope of the future work.

Finally, in contrast with the case of Marangoni convection in pure liquids at the present time there are no experimental studies on the Marangoni convection in thin layers of binary liquids available in the literature. Based on the importance of these systems in the process of crystal growth such experiments would be more than desirable. We hope that the results obtained in this paper will stimulate the researchers to carry out experiments with relevant binary liquid systems and to compare their findings with those presented here.

ACKNOWLEDGMENTS

The research was partially supported by the Israel Science Foundation founded by the Israel Academy of Sciences through Grant No. 31/03-15.3, the Smoler Research Fund, the Fund for the Promotion of Research at the Technion, and ICOPAC Research Network of the European Union (Contract No. HPRN-CT-2000-00136). A.A.N. acknowledges the support of the E. and J. Bishop Research Fund.

APPENDIX A: LINEAR STABILITY ANALYSIS—MONOTONIC INSTABILITY

The resulting set of equations and boundary conditions is written as

$$\tilde{\Psi}'''' - 2\epsilon^2 K^2 \tilde{\Psi}'' + \epsilon^4 K^4 \tilde{\Psi} = \overline{\omega}\epsilon^2 (\tilde{\Psi}'' - \epsilon^2 K^2 \tilde{\Psi}), \tag{A1a}$$

$$\tilde{T}'' - \epsilon^2 K^2 \tilde{T} = \overline{\omega}\epsilon^2 P \tilde{T} + i\epsilon^2 K \tilde{\Psi}, \tag{A1b}$$

$$\tilde{C}'' - \epsilon^2 K^2 \tilde{C} + \chi(\tilde{T}'' - \epsilon^2 K^2 \tilde{T}) = \overline{\omega}\epsilon^2 S \tilde{C} - i\epsilon^2 K \chi L^{-1} \tilde{\Psi}, \tag{A1c}$$

$$\tilde{\Psi} = 0, \quad \tilde{\Psi}' = 0, \quad \tilde{T}' = 0, \quad \tilde{C}' = 0 \quad \text{at} \quad z = 0, \tag{A1d}$$

$$\tilde{\Psi} = 0, \quad \tilde{T}' + \beta\epsilon^4 \tilde{T} = 0, \quad \tilde{C}' - \epsilon^4 \chi \beta \tilde{T} = 0,$$

$$\tilde{\Psi}'' + iK(M_0 + \epsilon^2 M_2 + \cdots)(\tilde{T} - \tilde{C}) = 0 \quad \text{at} \quad z = 1. \tag{A1e}$$

We integrate Eqs. (A1b) and (A1c) over the interval $0 \leqslant \eta \leqslant 1$ and the resulting integral relations serve us as solvability conditions

$$\epsilon^2 \overline{\omega} \begin{pmatrix} \langle P\tilde{T} \rangle \\ \langle S\tilde{C} \rangle \end{pmatrix} + iK\epsilon^2 \begin{pmatrix} 1 \\ -\chi L^{-1} \end{pmatrix} \langle \tilde{\Psi} \rangle + \epsilon^2 K^2 \begin{pmatrix} \langle \tilde{T} \rangle \\ \langle \tilde{C} + \chi \tilde{T} \rangle \end{pmatrix} = \epsilon^4 \beta \begin{pmatrix} -\tilde{T}|_{z=1} \\ 0 \end{pmatrix}, \tag{A2}$$

where $\langle f \rangle \equiv \int_0^1 f \, d\eta$.

At zeroth order of approximation one obtains

$$\Psi_0'''' = 0, \tag{A3a}$$

$$T_0'' = 0, \tag{A3b}$$

$$C_0'' + \chi T_0'' = 0, \tag{A3c}$$

$$\Psi_0 = 0, \ \Psi_0' = 0, \ T_0' = C_0' = 0 \quad \text{at} \quad z = 0, \tag{A3d}$$

$$\Psi_0 = 0, \quad \Psi_0'' + iKM_0(T_0 - C_0) = 0, \quad T_0' = 0, \quad C_0' = 0 \quad \text{at} \quad z = 1. \tag{A3e}$$

The solution of the problem, Eqs. (A3), is given by

$$\Psi_0 = \tfrac{1}{4} iKM_0(a_1 - a_2) z^2 (1 - z), \quad T_0 = a_1, \quad C_0 = a_2, \tag{A4}$$

where a_1 and a_2 are constants yet unknown to be determined later.

At second order the equations and boundary conditions read

$$\Psi_2'''' - 2K^2 \Psi_0'' = \omega_0 \Psi_0'', \tag{A5a}$$

$$T_2'' - K^2 T_0 = iK\Psi_0 + \omega_0 P T_0, \tag{A5b}$$

$$C_2'' - K^2 C_0 + \chi(T_2'' - K^2 T_0) = -iK\chi L^{-1} \Psi_0 + \omega_0 S C_0, \tag{A5c}$$

$$\Psi_2 = 0, \ \Psi_2' = 0, \ T_2' = 0, \ C_2' = 0 \quad \text{at} \quad z = 0, \tag{A5d}$$

$$\Psi_2 = 0, \quad \Psi_2'' + iKM_0(T_2 - C_2) + iKM_2(T_0 - C_0) = 0,$$

$$T_2' = 0, \ C_2' = 0 \quad \text{at} \quad z = 1. \tag{A5e}$$

The solvability condition, Eq. (A2), at second order of approximation yields

$$\mathbf{A}_1 \begin{pmatrix} a_1 \\ a_2 \end{pmatrix} = \begin{pmatrix} 0 \\ 0 \end{pmatrix} \quad \text{with} \quad \mathbf{A}_1 = \begin{pmatrix} \Lambda_0 P + 1 - m_0 & m_0 \\ -\Lambda_0 P \chi + m_0 \chi (1 + L^{-1}) & \Lambda_0 S + 1 - m_0 \chi (1 + L^{-1}) \end{pmatrix}, \tag{A6}$$

where $m_0 = M_0/48$ and $\omega_0 = \Lambda_0 K^2$.

Equation (A6) yields the relationship between the constants a_1 and a_2 in the form

$$a_2 = -\chi(1 + L^{-1}) a_1. \tag{A7}$$

In what follows we will choose $a_1 = 1$, so that $a_2 = -\chi(1 + L^{-1})$.

The solutions of Eqs. (A5) read

$$\Psi_2 = 48iK^3 (\tfrac{1}{24} z^4 - \tfrac{1}{40} z^5 - \tfrac{1}{60} z^3) + iK[12(b_1 - b_2) m_0 + \tfrac{1}{4} M_2 m_0^{-1}](z^2 - z^3), \tag{A8a}$$

$$T_2 = b_1 - 12K^2 (\tfrac{1}{12} z^4 - \tfrac{1}{20} z^5 - \tfrac{1}{24} z^2), \tag{A8b}$$

$$C_2 = b_2 + 12\chi(1 + L^{-1}) K^2 (\tfrac{1}{12} z^4 - \tfrac{1}{20} z^5 - \tfrac{1}{24} z^2), \tag{A8c}$$

where b_1 and b_2 are integration constants.

The solvability condition, Eq. (A2), at fourth order of approximation yields

$$\mathbf{A}_2 \begin{pmatrix} b_1 \\ b_2 \end{pmatrix} = \mathbf{r} \quad \text{with} \quad \mathbf{A}_2 = \begin{pmatrix} 1 - m_0 & m_0 \\ \chi(1 + m_0 L^{-1}) & 1 - \chi m_0 L^{-1} \end{pmatrix} \tag{A9}$$

and

$$\mathbf{r}\equiv\begin{pmatrix} r_1 \\ r_2 \end{pmatrix} = \begin{pmatrix} \dfrac{M_2}{48}m_0^{-1} - \dfrac{K^2}{15} - (P\omega_2+\beta)K^{-2} \\ -\dfrac{M_2}{48}\chi L^{-1}m_0^{-1} + \dfrac{K^2}{15}\chi L^{-1} + S\omega_2\chi(1+L^{-1})K^{-2} \end{pmatrix}. \tag{A10}$$

As operator $\mathbf{A}_2$ is singular, Eq. (A9) has a solution if and only if vector $\mathbf{r}$ is orthogonal to vector $\mathbf{s}$,

$$\mathbf{s}=\begin{pmatrix} 1+\chi \\ -1 \end{pmatrix}, \tag{A11}$$

being an eigenvector corresponding to a zero eigenvalue of the adjoint operator $\mathbf{A}_2^T$,

$$\mathbf{r}\cdot\mathbf{s}=0. \tag{A12}$$

APPENDIX B: LINEAR STABILITY ANALYSIS—OSCILLATORY INSTABILITY

The constants a_1 and a_2 in Eq. (A7) can be chosen as

$$a_1=1, \quad a_2=\frac{1-L^{-1}\chi-i\Omega_0 S(\chi+1)}{1+L^{-1}}. \tag{B1}$$

The solutions of Eqs. (A5) in the case of the oscillatory instability read

$$\begin{aligned}\Psi_2 = {} & iK^3(1+i\Omega_0 P)(2+i\Omega_0)\left(-\frac{3z^5}{5}+z^4\right) \\ & + iK^3(1+i\Omega_0 P)\left\{\frac{6}{5}\left[\frac{1+\chi(1+L^{-1}+L^{-2})}{L^{-1}(1+\chi)}-\frac{i\Omega_0}{2}\right]z^2\right. \\ & \left.-\left[\frac{6}{5}\frac{1+\chi(1+L^{-1}+L^{-2})}{L^{-1}(1+\chi)}+\frac{4}{5}-\frac{i\Omega_0}{5}\right]z^3\right\} \\ & +\left[\frac{12iK(1+L^{-1})}{L^{-1}(1+\chi)}(b_1-b_2)\right. \\ & \left.+\frac{iKM_2}{4}\frac{L^{-1}(1+\chi)(1+i\Omega_0 P)}{1+L^{-1}}\right](z^2-z^3),\end{aligned} \tag{B2a}$$

$$T_2=b_1-12K^2(1+i\Omega_0 P)\left(\tfrac{1}{12}z^4-\tfrac{1}{20}z^5-\tfrac{1}{24}z^2\right), \tag{B2b}$$

$$C_2=b_2+12\chi(1+L^{-1})K^2(1+i\Omega_0 P)\left(\tfrac{1}{12}z^4-\tfrac{1}{20}z^5-\tfrac{1}{24}z^2\right), \tag{B2c}$$

where b_1 and b_2 are integration constants.

APPENDIX C: LONGWAVE NONLINEAR STABILITY ANALYSIS—MONOTONIC INSTABILITY

In terms of the variables and parameters defined by Eq. (32), Eqs. (30) read

$$\epsilon^4\mathbf{U}_\tau+\epsilon^2P^{-1}[(\mathbf{U}\cdot\boldsymbol{\nabla})\mathbf{U}+W\partial_Z\mathbf{U}]=-\boldsymbol{\nabla}\Pi+\epsilon^2\nabla^2\mathbf{U}+\partial_{ZZ}\mathbf{U}, \tag{C1a}$$

$$\epsilon^4W_\tau+\epsilon^2P^{-1}[(\mathbf{U}\cdot\boldsymbol{\nabla})W+W\partial_Z W] = -\epsilon^{-2}\partial_Z\Pi+\epsilon^2\nabla^2W+\partial_{ZZ}W, \tag{C1b}$$

$$\boldsymbol{\nabla}\cdot\mathbf{U}+\partial_Z W=0, \tag{C1c}$$

$$\epsilon^4P\Theta_\tau+\epsilon^2(\mathbf{U}\cdot\boldsymbol{\nabla}\Theta+W\partial_Z\Theta-W)=\epsilon^2\nabla^2\Theta+\partial_{ZZ}\Theta, \tag{C1d}$$

$$\epsilon^4S\Sigma_\tau+\epsilon^2L^{-1}(\mathbf{U}\cdot\boldsymbol{\nabla}\Sigma+W\partial_Z\Sigma+\chi W) = \epsilon^2\nabla^2\Sigma+\partial_{ZZ}\Sigma+\chi\epsilon^2\nabla^2\Theta+\chi\partial_{ZZ}\Theta, \tag{C1e}$$

$$\mathbf{U}=W=\partial_Z\Theta=\partial_Z\Sigma=0 \quad \text{at} \quad Z=0, \tag{C1f}$$

$$W=\partial_Z\Sigma-\chi B\Theta=0, \quad \partial_Z\Theta+B\Theta=0,$$

$$\partial_Z\mathbf{U}+M\boldsymbol{\nabla}(\Theta-\Sigma)=\mathbf{0} \quad \text{at} \quad Z=1, \tag{C1g}$$

where hereafter $\boldsymbol{\nabla}\equiv(\partial_X,\partial_Y)$ and $\nabla^2=\partial_X^2+\partial_Y^2$.

We integrate Eqs. (C1d) and (C1e) over the interval $0\leqslant Z\leqslant 1$ and the resulting integral relations serve us as solvability conditions

$$P\epsilon^4\partial_\tau\langle\Theta\rangle+\epsilon^2\langle\boldsymbol{\nabla}\mathbf{U}\cdot\boldsymbol{\nabla}\Theta+W\partial_Z\Theta+W\rangle-\epsilon^2\langle\nabla^2\Theta\rangle -(\partial_Z\Theta)|_{Z=0}^{Z=1}=0, \tag{C2a}$$

$$S\epsilon^4\partial_\tau\langle\Sigma\rangle+\epsilon^2L^{-1}\langle\boldsymbol{\nabla}\mathbf{U}\cdot\boldsymbol{\nabla}\Sigma+W\partial_Z\Sigma+\chi W\rangle -\epsilon^2\langle\nabla^2\Sigma+\chi\nabla^2\Theta\rangle=0, \tag{C2b}$$

where here on $\langle f\rangle\equiv\int_0^1 f\,dZ$. It should be noted that the total contribution of the two terms containing the second derivatives with respect to Z in Eq. (C2) vanishes due to the boundary conditions at $Z=1$.

At zeroth order of approximation reckoning from Eq. (C1b) that $\partial_z\Pi^{(0)}=0$, one obtains

$$\partial_{ZZ}\mathbf{U}^{(0)}=\boldsymbol{\nabla}\Pi^{(0)}, \quad \partial_{ZZ}W^{(0)}=\partial_Z\Pi^{(2)}, \quad \boldsymbol{\nabla}\cdot\mathbf{U}^{(0)}+\partial_Z W^{(0)}=0, \tag{C3a}$$

$$\partial_{ZZ}\Theta^{(0)}=0, \quad \partial_{ZZ}\Sigma^{(0)}+\chi\partial_{ZZ}\Theta^{(0)}=0, \tag{C3b}$$

$$\mathbf{U}^{(0)}=0, \quad W^{(0)}=0, \quad \partial_Z\Theta^{(0)}=0, \quad \partial_Z\Sigma^{(0)}=0 \quad \text{at} \quad Z=0,$$

$$W^{(0)}=0, \quad \partial_Z\mathbf{U}^{(0)}+M_0\boldsymbol{\nabla}(\Theta^{(0)}-\Sigma^{(0)})=0, \quad \partial_Z\Theta^{(0)}=0,$$

$$\partial_Z\Sigma^{(0)}=0 \quad \text{at} \quad Z=1. \tag{C3c}$$

The solvability condition, Eq. (C2), at the zeroth order of approximation yields

$$\mathbf{A}\,\mathbf{V}=\begin{pmatrix}0\\0\end{pmatrix} \quad \text{with } \mathbf{A}=\begin{pmatrix}1-m_0 & m_0\\ \chi(1+L^{-1}m_0) & 1-\chi L^{-1}m_0\end{pmatrix},$$

$$\mathbf{V}=\nabla^2\begin{pmatrix}F\\G\end{pmatrix}. \tag{C4}$$

Equation (C4) yields the relationship between the functions F and G in the form

$$G=-\chi(1+L^{-1})[F-\langle\langle F\rangle\rangle], \tag{C5}$$

where $\langle\langle F\rangle\rangle=\mathcal{L}^{-1}\int\int F(X,Y,\tau)dXdY$ and the integration is carried out over the domain of periodicity in the X-Y plane of the area $\mathcal{L}$. The relationship (C5) shows that the average temperature disturbance per unit area $\langle\langle F\rangle\rangle$ may change in time due to imperfect insulation of the boundaries, however the average concentration disturbance per unit area $\ll G\gg=\mathcal{L}^{-1}\int\int G(X,Y,\tau)dXdY$ does not change in time in the absence of solute sources. It is noteworthy that Eq. (C5) follows from Eq. (C4) when the conditions of periodicity in the X-Y plane and boundedness of F and G are imposed.

At second order the equations and boundary conditions, Eqs. (C1), read

$$\partial_{ZZ}\mathbf{U}^{(2)}=-\nabla^2\mathbf{U}^{(0)}+\boldsymbol{\nabla}\Pi^{(2)}+P^{-1}[(\mathbf{U}^{(0)}\cdot\boldsymbol{\nabla})\mathbf{U}^{(0)}+W^{(0)}\partial_Z\mathbf{U}^{(0)}], \tag{C6a}$$

$$\partial_{ZZ}W^{(2)}=-\nabla^2W^{(0)}+\partial_Z\Pi^{(4)}+P^{-1}[(\mathbf{U}^{(0)}\cdot\boldsymbol{\nabla})W^{(0)}+W^{(0)}\partial_ZW^{(0)}], \tag{C6b}$$

$$\boldsymbol{\nabla}\cdot\mathbf{U}^{(2)}+\partial_ZW^{(2)}=0, \tag{C6c}$$

$$\partial_{ZZ}\Theta^{(2)}=-\nabla^2\Theta^{(0)}+(\mathbf{U}^{(0)}\cdot\boldsymbol{\nabla}\Theta^{(0)}+W^{(0)}\partial_Z\Theta^{(0)}-W^{(0)}), \tag{C6d}$$

$$\partial_{ZZ}\Sigma^{(2)}=-\nabla^2\Sigma^{(0)}-\chi(\nabla^2\Theta^{(0)}+\partial_{ZZ}\Theta^{(2)})+L^{-1}(\mathbf{U}^{(0)}\cdot\boldsymbol{\nabla}\Sigma^{(0)}+W^{(0)}\partial_Z\Sigma^{(0)}+\chi W^{(0)}), \tag{C6e}$$

$$\mathbf{U}^{(2)}=\mathbf{0}, \quad W^{(2)}=0, \quad \partial_Z\Theta^{(2)}=0, \quad \partial_Z\Sigma^{(2)}=0 \quad \text{at} \quad Z=0, \tag{C6f}$$

$$W^{(2)}=0,$$

$$\partial_Z\mathbf{U}^{(2)}+M_0\boldsymbol{\nabla}(\Theta^{(2)}-\Sigma^{(2)})+M_2\boldsymbol{\nabla}(\Theta^{(0)}-\Sigma^{(0)})=\mathbf{0},$$

$$\partial_Z\Theta^{(2)}=0, \quad \partial_Z\Sigma^{(2)}=0 \quad \text{at} \quad Z=1. \tag{C6g}$$

The solutions of Eqs. (C6) read

$$\Theta^{(2)}=Q(X,Y,\tau)+(\tfrac{1}{6}-\tfrac{1}{2}Z^2)\nabla^2F+m_0p_3\boldsymbol{\nabla}H\cdot\boldsymbol{\nabla}F+m_0p_4\nabla^2H, \tag{C7a}$$

$$\Sigma^{(2)}=R(X,Y,\tau)+(\tfrac{1}{6}-\tfrac{1}{2}Z^2)\nabla^2(\chi F+G)+m_0L^{-1}p_3\boldsymbol{\nabla}G\cdot\boldsymbol{\nabla}H-\chi L^{-1}m_0p_4\nabla^2H-\chi\Theta^{(2)}, \tag{C7b}$$

$$\mathbf{U}^{(2)}=\left(\frac{1}{2}Z^2-Z\right)\boldsymbol{\nabla}J+24m_0p_5\boldsymbol{\nabla}\nabla^2H+Z\boldsymbol{\nabla}[48m_0R-48m_0(1+\chi)Q-M_2H]+\frac{72m_0^2}{P}p_6\boldsymbol{\nabla}(|\boldsymbol{\nabla}H|^2)+\frac{144m_0^2}{P}p_7\boldsymbol{\nabla}H\nabla^2H+\frac{144m_0^2}{5}Z[L^{-1}\boldsymbol{\nabla}(\boldsymbol{\nabla}H\cdot\boldsymbol{\nabla}G)-(1+\chi)\boldsymbol{\nabla}(\boldsymbol{\nabla}H\cdot\boldsymbol{\nabla}F)], \tag{C7c}$$

$$W^{(2)}=-\frac{2}{5}m_0p_8\nabla^4H+Z^2\nabla^2\left[\frac{1}{2}M_2H+24m_0\{(1+\chi)Q-R\}\right]-\frac{12m_0^2}{35P}[p_9\nabla^2(|\boldsymbol{\nabla}H|^2)+p_2\boldsymbol{\nabla}\cdot(\nabla^2H\boldsymbol{\nabla}H)]+\frac{72m_0^2}{5}Z^2\nabla^2[(1+\chi)(\boldsymbol{\nabla}H\cdot\boldsymbol{\nabla}F)-L^{-1}(\boldsymbol{\nabla}H\cdot\boldsymbol{\nabla}G)]+p_1\nabla^2J, \tag{C7d}$$

$$\Pi^{(2)}=12m_0(3Z^2-2Z)\nabla^2H+J, \tag{C7e}$$

where $H=F-G$,

$$p_1=\tfrac{1}{2}Z^2-\tfrac{1}{6}Z^3, \quad p_2=-14Z^5+28Z^6-12Z^7-28Z^2,$$

$$p_3=4Z^3-3Z^4-\tfrac{2}{5}, \quad p_4=Z^4-\tfrac{3}{5}Z^5-\tfrac{1}{10},$$

$$p_5=\tfrac{1}{4}Z^4-\tfrac{1}{3}Z^3+\tfrac{1}{15}Z, \quad p_6=\tfrac{1}{3}Z^4-\tfrac{3}{5}Z^5+\tfrac{3}{10}Z^6-\tfrac{2}{15}Z,$$

$$p_7=-\tfrac{1}{6}Z^4+\tfrac{2}{5}Z^5-\tfrac{1}{5}Z^6-\tfrac{2}{15}Z,$$

$$p_8=3Z^5-5Z^4+2Z^2, \quad p_9=14Z^5-21Z^6+9Z^7-14Z^2,$$

and $J\equiv J(X,Y,\tau)$, which satisfies the equation

$$\nabla^2J=-\frac{m_0^2}{35P}[432\nabla^2(|\boldsymbol{\nabla}H|^2)+936\boldsymbol{\nabla}\cdot(\nabla^2H\boldsymbol{\nabla}H)]-\tfrac{3}{2}M_2\nabla^2H+72m_0\nabla^2[R-(1+\chi)Q]+\tfrac{216}{5}m_0^2\nabla^2[L^{-1}\boldsymbol{\nabla}H\cdot\boldsymbol{\nabla}G-(1+\chi)\boldsymbol{\nabla}H\cdot\boldsymbol{\nabla}F]. \tag{C8}$$

The solvability condition, Eq. (C2), at fourth order in ϵ written in vector form yields

$$\begin{pmatrix} 0 \\ 0 \end{pmatrix} = \partial_\tau \begin{pmatrix} PF \\ SG \end{pmatrix} + \begin{pmatrix} \beta\Theta^{(0)} \\ 0 \end{pmatrix} + \begin{pmatrix} \langle \mathbf{U}^{(0)} \cdot \boldsymbol{\nabla}\Theta^{(2)} + W^{(0)}\partial_Z\Theta^{(2)} - W^{(2)} + \boldsymbol{\nabla}\Theta^{(0)} \cdot \mathbf{U}^{(2)} - \nabla^2\Theta^{(2)} \rangle \\ \langle L^{-1}(\mathbf{U}^{(0)} \cdot \boldsymbol{\nabla}\Sigma^{(2)} + W^{(0)}\partial_Z\Sigma^{(2)} + \chi W^{(2)} + \boldsymbol{\nabla}\Sigma^{(0)} \cdot \mathbf{U}^{(2)}) - \nabla^2(\Sigma^{(2)} + \chi\Theta^{(2)}) \rangle \end{pmatrix}. \quad \text{(C9)}$$

Equation (C9) can be recast into the form

$$\mathbf{A}_2 \quad \nabla^2 \begin{pmatrix} Q \\ R \end{pmatrix} = \mathbf{r}, \quad \text{(C10)}$$

where

$$\mathbf{A}_2 = \begin{pmatrix} 1 - m_0(1+\chi) & m_0 \\ m_0\chi(1+\chi)L^{-1} & 1 - m_0\chi L^{-1} \end{pmatrix}. \quad \text{(C11)}$$

The Fredholm alternative for Eqs. (C4) and (C10) yields the orthogonality of vectors $\mathbf{r}$ and $\mathbf{s}$,

$$\mathbf{r} \cdot \mathbf{s} = 0 \quad \text{where } \mathbf{s} = \begin{pmatrix} 1+\chi \\ -1 \end{pmatrix} \phi(X, Y, \tau) \quad \text{(C12)}$$

is the eigenvector corresponding to a zero eigenvalue of the adjoint operator $\mathbf{A}_2^T$.

Equation (C8) can be rewritten as

$$\begin{aligned} \boldsymbol{\nabla} J = & -\frac{m_0^2}{35P}[432\boldsymbol{\nabla}(|\boldsymbol{\nabla}H|^2) + 936\nabla^2 H \boldsymbol{\nabla}H - \tfrac{3}{2}M_2\boldsymbol{\nabla}H \\ & + 72m_0\boldsymbol{\nabla}[R - (1+\chi)Q] \\ & + \tfrac{216}{5}m_0^2\boldsymbol{\nabla}[L^{-1}\boldsymbol{\nabla}H \cdot \boldsymbol{\nabla}G - (1+\chi)\boldsymbol{\nabla}H \cdot \boldsymbol{\nabla}F] + \hat{\mathbf{J}}, \end{aligned} \quad \text{(C13)}$$

where $\boldsymbol{\nabla} \cdot \hat{\mathbf{J}} = 0$. The vector $\hat{\mathbf{J}}$ is divergence-free and two-dimensional, and thus can be written in terms of a single function $E \equiv E(X, Y, \tau)$ as $\hat{\mathbf{J}} = (\partial_Y E, -\partial_X E)$.

APPENDIX D: LONG-WAVELENGTH NONLINEAR STABILITY ANALYSIS-OSCILLATORY INSTABILITY

Equations (62) are rewritten in the rescaled variables up to $O(\epsilon^4)$ terms in the following form:

$$\begin{aligned} & \epsilon^2\Psi_{ZZT} + \epsilon^4(\Psi_{ZZ\tau} + \Psi_{XXT}) + P^{-1}[\epsilon^2(\Psi_Z\Psi_{ZZX} - \Psi_X\Psi_{ZZZ}) \\ & \quad + \epsilon^4(\Psi_Z\Psi_{XXX} - \Psi_X\Psi_{XXZ})] \\ & = \Psi_{ZZZZ} + 2\epsilon^2\Psi_{XXZZ} + \epsilon^4\Psi_{XXXX}, \end{aligned} \quad \text{(D1a)}$$

$$\begin{aligned} & \epsilon^2 P\Theta_T + \epsilon^4 P\Theta_\tau + \epsilon^2\Psi_Z\Theta_X - \epsilon^2\Psi_X\Theta_Z + \epsilon^2\Psi_X \\ & \quad = \epsilon^2\Theta_{XX} + \Theta_{ZZ}, \end{aligned} \quad \text{(D1b)}$$

$$\begin{aligned} & \epsilon^2[S\Sigma_T + L^{-1}(\Psi_Z\Sigma_X - \Psi_X\Sigma_Z - \chi\Psi_X)] + \epsilon^4 S\Sigma_\tau \\ & \quad = \epsilon^2\Sigma_{XX} + \Sigma_{ZZ} + \chi(\epsilon^2\Theta_{XX} + \Theta_{ZZ}), \end{aligned} \quad \text{(D1c)}$$

$$\Psi = \Psi_Z = \Theta_Z = \Sigma_Z = 0 \quad \text{at} \quad Z = 0, \quad \text{(D1d)}$$

$$\begin{aligned} & \Psi = \Sigma_Z - \epsilon^4\chi\beta\Theta = 0, \quad \Theta_Z + \epsilon^4\beta\Theta = 0, \quad \Psi_{ZZ} + M(\Theta_X \\ & \quad - \Sigma_X) = 0 \quad \text{at} \quad Z = 1. \end{aligned} \quad \text{(D1e)}$$

The boundary-value problem, Eqs. (D1), is solved using the asymptotic expansion in the form Eq. (33). At zeroth order of approximation we obtain

$$\Psi^{(0)}_{ZZZZ} = 0, \quad \text{(D2a)}$$

$$\Theta^{(0)}_{ZZ} = 0, \quad \text{(D2b)}$$

$$\Sigma^{(0)}_{ZZ} + \chi\Theta^{(0)}_{ZZ} = 0, \quad \text{(D2c)}$$

$$\Psi^{(0)} = 0, \quad \Psi^{(0)}_Z = 0, \quad \Theta^{(0)}_Z = 0, \quad \Sigma^{(0)}_Z = 0 \quad \text{at} \quad Z = 0, \quad \text{(D2d)}$$

$$\Psi^{(0)} = 0, \quad \Psi^{(0)}_{ZZ} + M_0(\Theta^{(0)}_X - \Sigma^{(0)}_X) = 0, \quad \Theta^{(0)}_Z = 0,$$
$$\Sigma^{(0)}_Z = 0 \quad \text{at} \quad Z = 1. \quad \text{(D2e)}$$

At second order the boundary-value problem reads

$$\Psi^{(2)}_{ZZZZ} + 2\Psi^{(0)}_{XXZZ} = \Psi^{(0)}_{ZZT} + P^{-1}(\Psi^{(0)}_Z\Psi^{(0)}_{ZZX} - \Psi^{(0)}_X\Psi^{(0)}_{ZZZ}), \quad \text{(D3a)}$$

$$\Theta^{(2)}_{ZZ} + \Theta^{(0)}_{XX} = P\Theta^{(0)}_T + \Psi^{(0)}_Z\Theta^{(0)}_X + \Psi^{(0)}_X, \quad \text{(D3b)}$$

$$\begin{aligned} & \Sigma^{(2)}_{ZZ} + \Sigma^{(0)}_{XX} + \chi(\Theta^{(2)}_{ZZ} + \Theta^{(0)}_{XX}) \\ & \quad = S\Sigma^{(0)}_T + SP^{-1}(\Psi^{(0)}_Z\Sigma^{(0)}_X - \chi\Psi^{(0)}_X), \end{aligned} \quad \text{(D3c)}$$

$$\Psi^{(2)} = 0, \quad \Psi^{(2)}_Z = 0, \quad \Theta^{(2)}_Z = 0, \quad \Sigma^{(2)}_Z = 0 \quad \text{at} \quad Z = 0, \quad \text{(D3d)}$$

$$\Psi^{(2)} = 0, \quad \Psi^{(2)}_{ZZ} + M_0(\Theta^{(2)}_X - \Sigma^{(2)}_X) + M_2(\Theta^{(0)}_X - \Sigma^{(0)}_X) = 0,$$
$$\Theta^{(2)}_Z = 0, \quad \Sigma^{(2)}_Z = 0 \quad \text{at} \quad Z = 1. \quad \text{(D3e)}$$

The solvability condition for the subsystem of equations and boundary conditions determining $\Theta^{(2)}$ and $\Sigma^{(2)}$ gives the following leading-order amplitude equations that govern the evolution of the temperature and concentration disturbances, F and G, on the time scale $T = \epsilon^2 t$,

$$F_T = -P^{-1}(m_0 - 1)F_{XX} + m_0P^{-1}G_{XX}, \quad \text{(D4)}$$

$$G_T = \chi(S^{-1} + m_0P^{-1})F_{XX} + (S^{-1} - \chi m_0P^{-1})G_{XX}, \quad \text{(D5)}$$

where $m_0 = M_0/48$. This linear system of equations reproduces the results of the linear stability analysis, Eq. (27).

The solution of the boundary-value problem (D3) reads

$$\Theta^{(2)}=Q(X,T,\tau)+m_0\left(-\frac{3}{5}Z^5+Z^4-\frac{1}{2}Z^2+\frac{1}{15}\right)\times(F_{XX}-G_{XX})+m_0\left(-3Z^4+4Z^3-\frac{2}{5}\right)F_X(F_X-G_X), \tag{D6a}$$

$$\Sigma^{(2)}=R(X,T,\tau)+\chi(1+L^{-1})m_0\left(\frac{3}{5}Z^5-Z^4+\frac{1}{2}Z^2-\frac{1}{15}\right)\times(F_{XX}-G_{XX})+m_0P^{-1}\left(-3Z^4+4Z^3-\frac{2}{5}\right)\times(F_X-G_X)(SG_X-\chi PF_X), \tag{D6b}$$

$$\Psi^{(2)}=\frac{Z^3-Z^2}{140P}\{G_X[35M_2P+48m_0^2(19+21S+21P(1+\chi)+q_1(Z))F_{XX}-48m_0^2(19+42S+q_1(Z))G_{XX}]+F_X[-35M_2P-48m_0^2(19+42P(1+\chi)+q_1(Z))F_{XX}+48m_0^2(19+21S+21P(1+\chi)+q_1(Z))G_{XX}]+28m_0[60P(R_X-Q_X)+Pq_2(Z)((P^{-1}-\chi S^{-1})F_{XXX}-S^{-1}G_{XXX})-(2Pq_2(Z)-2Pm_0(1+\chi+\chi L^{-1})+m_0(1+\chi)q_2(Z))(F_{XXX}-G_{XXX})]\}, \tag{D6c}$$

where $q_1(Z)=-6Z-6Z^2+8Z^3-6Z^4$, $q_2(Z)=3+2Z-3Z^2$, $Q(X,T,\tau)$, and $R(X,T,\tau)$ are unknown functions.

At fourth order we shall write only the boundary-value problem for $\Theta^{(4)}$ and $\Sigma^{(4)}$,

$$\Theta^{(4)}_{ZZ}+\Theta^{(2)}_{XX}=P\Theta^{(2)}_T+P\Theta^{(0)}_\tau+\Psi^{(2)}_Z\Theta^{(0)}_X+\Psi^{(0)}_Z\Theta^{(2)}_X-\Psi^{(0)}_X\Theta^{(2)}_Z+\Psi^{(2)}_X, \tag{D7a}$$

$$\Sigma^{(4)}_{ZZ}+\Sigma^{(2)}_{XX}+\chi(\Theta^{(4)}_{ZZ}+\Theta^{(2)}_{XX})=S\Sigma^{(2)}_T+S\Sigma^{(0)}_\tau+L^{-1}(\Psi^{(2)}_Z\Sigma^{(0)}_X+\Psi^{(0)}_Z\Sigma^{(2)}_X-\Psi^{(0)}_X\Sigma^{(2)}_Z-\chi\Psi^{(2)}_X), \tag{D7b}$$

$$\Theta^{(4)}_Z=0,\quad \Sigma^{(4)}_Z=0 \qquad \text{at} \quad Z=0, \tag{D7c}$$

$$\Theta^{(4)}_Z+\beta\Theta^{(0)}=0,\quad \Sigma^{(4)}_Z-\chi\beta\Theta^{(0)}=0 \quad \text{at} \quad Z=1. \tag{D7d}$$

Integrating equations over Z and using the boundary conditions, we arrive to the following solvability conditions:

$$PF_\tau+P\langle\Theta^{(2)}\rangle_T+\langle\Psi^{(2)}\rangle_X+\langle\Psi^{(0)}_Z\Theta^{(2)}\rangle_X-\langle\Theta^{(2)}\rangle_{XX}+\beta F=0, \tag{D8}$$

$$SG_\tau+S\langle\Sigma^{(2)}\rangle_T-L^{-1}\chi\langle\Psi^{(2)}\rangle_X+L^{-1}\langle\Psi^{(0)}_Z\Sigma^{(2)}\rangle_X-\langle\Sigma^{(2)}\rangle_{XX}-\chi\langle\Theta^{(2)}\rangle_{XX}=0, \tag{D9}$$

where the identity

$$\langle\Psi_Z\Theta_X-\Psi_X\Theta_Z\rangle=\langle\Psi_Z\Theta\rangle_X$$

was used to simplify the algebraic derivations.

[1] S. Ostrach, J. Fluids Eng. **105**, 5 (1983), and references therein.
[2] D.A. Nield, J. Fluid Mech. **29**, 545 (1967).
[3] E. Knobloch, Phys. Rev. A **40**, 1549 (1989).
[4] J.S. Turner, Annu. Rev. Fluid Mech. **6**, 37 (1974).
[5] J.S. Turner, Annu. Rev. Fluid Mech. **17**, 11 (1985).
[6] M.C. Cross and P.C. Hohenberg, Rev. Mod. Phys. **65**, 851 (1993).
[7] S.H. Davis, Annu. Rev. Fluid Mech. **19**, 403 (1987), and references therein.
[8] J.L. Castillo and M.G. Velarde, Phys. Lett. **66A**, 489 (1978).
[9] J.L. Castillo and M.G. Velarde, J. Non-Equilib. Thermodyn. **5**, 111 (1980).
[10] J.L. Castillo and M.G. Velarde, J. Fluid Mech. **125**, 463 (1982).
[11] C.L. McTaggart, J. Fluid Mech. **134**, 301 (1983).
[12] C.F. Chen and C.C. Chen, Phys. Fluids **6**, 1482 (1994).
[13] J.K. Bhattacharjee, Phys. Rev. E **50**, 1198 (1994).
[14] J.R.L. Skarda, D. Jacqmin, and F.E. McCaughan, J. Fluid Mech. **366**, 109 (1998).
[15] S. Slavchev, G. Simeonov, S. Van Vaerenbergh, and J.C. Legros, Int. J. Heat Mass Transfer **42**, 3007 (1999).
[16] P.L. Garcia-Ybarra and M.G. Velarde, Phys. Fluids **30**, 1649 (1987).
[17] K.-L. Ho and H.-C. Chang, AIChE J. **34**, 705 (1988).
[18] A. Bergeon, D. Henry, H. Benhadid, and L.S. Tuckerman, J. Fluid Mech. **375**, 143 (1998).
[19] M. Bestehorn and P. Colinet, Physica D **145**, 84 (2000).
[20] J. Tanny, C.C. Chen, and C.F. Chen, J. Fluid Mech. **303**, 1 (1995).
[21] L. Braverman and A. Oron, J. Eng. Math. **32**, 343 (1997).
[22] G.I. Sivashinsky, Physica D **4**, 227 (1982).

[23] A. Oron and P. Rosenau, Phys. Rev. A **39**, 2063 (1989).
[24] E. Knobloch, Physica D **41**, 450 (1990).
[25] L. Shtilman and G.I. Sivashinsky, Physica D **52**, 477 (1991).
[26] A.A. Golovin, A.A. Nepomnyashchy, and L.M. Pismen, Physica D **81**, 117 (1995).
[27] D. Hefer and L.M. Pismen, Phys. Fluids **30**, 2648 (1987).
[28] L.M. Pismen, Phys. Rev. A **38**, 2564 (1988).
[29] S.M. Cox, J. Eng. Math. **28**, 463 (1994).
[30] J.R.A. Pearson, J. Fluid Mech. **4**, 489 (1958).
[31] A.A. Golovin, A.A. Nepomnyashchy, and L.M. Pismen, Int. J. Bifurcation Chaos **12**, 2487 (2002).
[32] A.A. Nepomnyashchy, M.G. Velarde, and P. Colinet, *Interfacial Phenomena and Convection* (Chapman & Hall, London/CRC, Boca Raton, 2002).